Supplementary Information for

Ecological networks of dissolved organic matter and microorganisms under global change

The file includes:

Supplementary Methods

Supplementary Tables (S1–S5)

Supplementary Figures (S1–S21)

Supplementary Methods

Considerations of the experimental design

In our study, we took advantage of elevational temperature gradients as a natural experiment. Natural climatic gradients along latitudinal and elevational gradients have played a pivotal role in testing the importance of climatic factors on biological community composition in the history of biogeography not only for macroorganisms, but also for microorganisms and biogeochemical cycling, and experimental manipulations along elevational or biogeographical gradients have been recognised as an important tool for disentangling different underlying drivers on community structure and ecosystem processes. For instance, De Sassi *et al.* [1] used a natural temperature gradient along elevations, combined with experimental nitrogen fertilization, to investigate the effects of elevated temperature and globally increasing anthropogenic nitrogen deposition on the structure and phenology of a grassland herbivore assemblage. Thus, using manipulative experiments along broad environmental gradients can help tease apart the relative importance of the interactive effects of local-scale factors and broad-scale climatic variation in shaping biological communities and ecosystem processes.

Temperature generally correlates strongly negatively with elevation, which was also true in our study showing significantly negatively correlation between measured water temperature and elevation in both China and Norway ($R^2 = 0.98$, $P < 0.05$, and $R^2 = 0.96$, $P < 0.05$, respectively). Specifically, we used the common sediment from Taihu Lake at each elevation with ten nutrient levels, and microbes from the local species pool of each elevation could be inoculated into the common sediment. As such, the covariance between climate and natural environments such as nutrients could be eliminated, which could disentangle the independent effects of temperature versus nutrient enrichment and also their interactive effects on the associations between DOM and microbes. Similar achievements are also reported in previous literature by experiments on mountainsides. For instance, in a translocation experiment, microbial decomposers were deliberately inoculated onto common leaf litter to disentangle the effects of microbial community versus temperature on litter decomposition rates and reevaluate the role of microbial community composition in its decomposition responses to climate [2].

However, for in-situ experiments, it is inevitable that there are some unmeasured environmental variables which might have some effects on biological communities and ecosystem processes. This will not be a major problem if our main focus was to investigate the major environmental variables which are playing pivotal roles in structuring biological and organic carbon compositions. Our data support that temperature and nutrients were key factors in explaining chemodiversity and bacterial community composition [3]. In our study, we considered as many important environmental variables as possible, such as chlorophyll *a*, bacterial abundance and nutrients. Due to practical and logistical issues, we were unable to measure all potential variables, such as UV radiation, across all elevations. This is largely because we have no clear evidence that these other variables have a dominant role in affecting the sediment bacterial and DOM compositions we studied here. More importantly, the bottom of our microcosm was buried into the local soils by 10% of the bottle height, and so sediments of each bottle were below the ground surface. It is thus unlikely that UV radiation and the related photodegradation would have stronger effects on bacteria and DOM in the sediments than temperature and nutrients.

In addition to relying on natural temperature gradients, controlled temperature experiments are another option to study climate effects on biological communities or organic matter decomposition. So far, there are two primary tools for simulating warming: passive greenhouses and active heating devices including soil, water and aerial arrays. Generally, controlling water temperatures in the field will encounter serious practical issues on mountainsides along large geographical regions. For instance, to prevent malfunction in a long-term run, heating devices are needed to be checked and replaced regularly, which is not possible in remote mountains and high elevations as in our current study. To obtain desired temperatures is also not easy in the field due to the variations such as in wind velocities, sun shine and forest shading along elevations. We do not see clearly how to practically and efficiently control for water temperatures in such a large-scale field study, and thus relied on natural temperature gradients.

It should be noted that our aims were considered to be as realistic as possible by combining field experiments and natural gradients, and by considering only the most

important and generally most interesting factors (that is, nutrients and temperature) for robust findings. Compared to field experiments, researchers can much more easily control virtually all aspects important for biological communities and organic matter in laboratory experiments. But laboratory experiments can be also easily criticized by some researchers to be far from realistic and results may not be applicable for real natural communities [4]. Different from laboratory manipulations, we think that these experiments are closer to nature environments, and expect such experiments to bridge between laboratory experiments and field observations. The communities in the microcosms should be dynamically driven by ecological processes, such as species dispersal, growth and extinction, and a time-series sampling would be ideally helpful to capture these processes. However, considering the harsh field situations in remote mountains or high elevations, the nature of destructive sampling, the large sample volumes required for repeat sampling, and the limited resources, it is unlikely we could have sampled biological communities and DOM at more than one time-point. As a tradeoff among logistics issue, heavy workload and robust results, we only sampled once after a one-month field incubation, and are confident that a final number of 300 DOM or bacterial samples across two mountains, 10 elevations and 10 nutrient levels was large enough for solid statistical analyses. We welcome future studies to undertake more intensive experiments if more resources could be allocated.

Supplementary Tables

Table S1. Variables used to explain the specialization of DOM-bacteria interactions. These variables were considered based on the hypothetical casual relationships in Fig. 6a: climate change, human impacts and contemporary nutrient variables as distal drivers, and energy supply, biodiversity, chemodiversity and DOM traits as proximal drivers. NMDS: non-metric multidimensional scaling.

Drivers	Group	Subgroup	Variable	Description
Distal drivers	Environment	Climate change	Temp	Water temperature[#1]
		Human impacts	ADD.NO_3	Nutrient enrichment[#2]
		Contemporary nutrient	TN.sedi	Sediment total nitrogen (TN)
		Contemporary nutrient	TP.sedi	Sediment total phosphorus (TP)
		Contemporary nutrient	NO_x.sedi	Sediment NO_x^-
		Contemporary nutrient	NO_2.sedi	Sediment NO_2^-
		Contemporary nutrient	NH_4.sedi	Sediment NH_4^+
		Contemporary nutrient	PO_4.sedi	Sediment PO_4^{3-}
		Contemporary nutrient	NO_3	Water NO_3^-
		Contemporary nutrient	NO_2	Water NO_2^-
		Contemporary nutrient	NH_4	Water NH_4^+
		Contemporary nutrient	PO_4	Water PO_4^{3-}
Proximal drivers	Energy supply	Energy supply	TC.sedi	Sediment total organic carbon (TOC)
		Energy supply	DOC.sedi	Sediment dissolved organic carbon (DOC)
		Energy supply	pH	Water pH
		Energy supply	Chla.sedi	Sediment Chlorophyll *a* (Chl *a*)
	Diversity	Biodiversity	bac.rich	Species richness of bacteria
		Biodiversity	bac.nmds1	NMDS axis 1 of bacterial composition
		Biodiversity	bac.nmds2	NMDS axis 2 of bacterial composition
		Chemodiversity	chemo.rich	Chemical richness of molecules
		Chemodiversity	mol.nmds1	NMDS axis 1 of molecular composition
		Chemodiversity	mol.nmds2	NMDS axis 2 of molecular composition
	Molecular traits	Molecular weight	Mass	The mass to charge ratio (m/z)
		Molecular weight	C	The number of carbon
		Molecular weight	$kdefect_{CH2}$	Kendrick Defect
		Stoichiometry	O/C	O/C ratio
		Stoichiometry	H/C	H/C ratio
		Stoichiometry	N/C	N/C ratio
		Stoichiometry	P/C	P/C ratio
		Stoichiometry	N/P	N/P ratio
		Stoichiometry	S/C	S/C ratio

	Chemical structure	AI_{Mod}	The modified aromaticity index
	Chemical structure	DBE	Double bond equivalence
	Chemical structure	DBE_O	Double bond equivalence minus oxygen
	Chemical structure	DBE_{AI}	Double bond equivalence minus aromaticity index
	Oxidation state	GFE	Gibbs free energy
	Oxidation state	NOSC	Nominal oxidation state of carbon
	Carbon use efficiency	Y_{met}	Carbon use efficiency

[#1] Water temperature was used to represent climatic variables due to its strong relations with elevation in both mountain ranges (Wang *et al*. 2016).

[#2] Nitrate addition ($ADD.NO_3$) was used to represent nutrient enrichment as the ratio between nitrate and phosphorus in the initial overlying water was constant.

Table S2. Variables used to explain DOM features. These variables were categorised into three groups: Environment (climate change, human impacts and contemporary nutrient), energy supply and biodiversity. NMDS: non-metric multidimensional scaling.

Group	Subgroup	Variable	Description
Environment	Climate change	Temp	Water temperature
	Human impacts	ADD.NO_3	Nutrient enrichment
	Contemporary nutrient	TN.sedi	Sediment total nitrogen (TN)
	Contemporary nutrient	TP.sedi	Sediment total phosphorus (TP)
	Contemporary nutrient	NO_x.sedi	Sediment NO_x^-
	Contemporary nutrient	NO_2.sedi	Sediment NO_2^-
	Contemporary nutrient	NH_4.sedi	Sediment NH_4^+
	Contemporary nutrient	PO_4.sedi	Sediment PO_4^{3-}
	Contemporary nutrient	NO_3	Water NO_3^-
	Contemporary nutrient	NO_2	Water NO_2^-
	Contemporary nutrient	NH_4	Water NH_4^+
	Contemporary nutrient	PO_4	Water PO_4^{3-}
Energy supply	Energy supply	TC.sedi	Sediment total organic carbon (TOC)
	Energy supply	DOC.sedi	Sediment dissolved organic carbon (DOC)
	Energy supply	pH	Water pH
	Energy supply	Chla.sedi	Sediment Chlorophyll *a* (Chl *a*)
Biodiversity	Biodiversity	bac.rich	Species richness of bacteria
	Biodiversity	bac.nmds1	NMDS axis 1 of bacterial composition
	Biodiversity	bac.nmds2	NMDS axis 2 of bacterial composition

Table S3. Formulae to calculate composite variables for structure equation models of the specialization H_2' of DOM-bacteria interactions. We constructed four bipartite networks, that is, the negative and positive interaction networks in China or Norway. The obtained composite variables were used in Fig. 6. The abbreviations of included variables are listed in Table S1.

Response	Region	Network type	Composite	Formula
H_2'	China	Negative	Contemporary nutrient	-0.606 × NO_3 + -0.222 × NO_2 + 0.221 × PO_4 + -0.294 × TN.sedi + 0.184 × PO_4.sedi + 0.296 × NH_4.sedi + 0.219 × NO_2.sedi
			Energy supply	-0.589 × pH + 0.493× DOC.sedi
			Biodiversity	-0.278 × bac.nmds1 + 0.160 × bac.nmds2
			Chemodiversity	-0.451× chemo.rich + 0.481 × mol.nmds1
			Molecular traits	66.076 × Mass + -64.710 × C + -1.402 × AI_{Mod} + -15.166 × DBE + -20.154 × DBE_O + 61.402 × DBE_{AI} + -3.279 × GFE + -23.908 × $kdefect_{CH2}$ + -1.378 × O/C + 2.627 × H/C + 0.652 × N/P
H_2'	China	Positive	Contemporary nutrient	0.339 × NO_2 + -0.442 × PO_4 + 0.443 × PO_4.sedi + -0.173 × NO2.sedi
			Energy supply	0.525 × pH + 0.253 × Chla.sedi + -0.102 × TC.sedi + -0.262 × DOC.sedi
			Biodiversity	-0.293 × bac.rich + 0.718 × bac.nmds1
			Chemodiversity	-0.110 × chemo.rich + -0.591 × mol.nmds1 + 0.416 × mol.nmds2
			Molecular traits	-50.009 × Mass + 48.984 × C + 1.728 × AI_{Mod} + 3.075 × DBE_O + -26.770 × DBE_{AI} + 3.904 × GFE + 24.822 × $kdefect_{CH2}$ + 1.204 × O/C + -5.311 × H/C
H_2'	Norway	Negative	Contemporary nutrient	-0.381 × NO_3 + 0.365 × PO_4.sedi
			Energy supply	0.210 × DOC.sedi
			Chemodiversity	-0.359 × chemo.rich + -0.186 × mol.nmds1 + -0.120 × mol.nmds2
			Molecular traits	-1.316 × Mass + 1.062 × AI_{Mod} + 3.571 × DBE + 2.524 × DBE_O + -4.638 × DBE_{AI} + 2.193 × H/C + -0.387 × N/C + -0.372 × N/P
H_2'	Norway	Positive	Contemporary nutrient	-0.338 × NO_3 + 0.280 × NO_2 + 0.338 × PO_4 + 0.350 × PO_4.sedi + -0.105 × NO_2.sedi
			Energy supply	-0.327 × pH + 0.231 × TC.sedi + -0.350 × DOC.sedi
			Biodiversity	-0.510 × bac.nmds1
			Chemodiversity	-0.169 × mol.nmds1 + -0.480 × mol.nmds2
			Molecular traits	1.872 × Mass + -1.825 × DBE + 2.282 × DBE_{AI} + -2.674 × GFE + -1.431 × $kdefect_{CH2}$ + 1.288 × H/C + -0.877 × N/C + 1.653 × P/C

Table S4. Summary of the model fit statistics evaluated for standardized structural equation model (SEM). We explored the potential links between predictor variables and the specialization H_2' of the negative and positive bipartite networks in China or Norway, and the best-fitting models are shown in Fig. 6. We constructed the full SEM models based on the hypothetical casual relationships (Fig. 6a), and further performed sequential models by dropping non-significant paths from the full models. χ^2: Chi-square. *P*: p-value of chi-square test. df: Degrees of freedom. CFI: Comparative fit index. SRMR: Standardized root mean squared residual. AICc: Second-order Akaike information criterion. ΔAICc: Delta AICc.

SEM models	Omitted paths	df	χ^2	*P*	CFI	SRMR	AICc	ΔAICc
China; Negative								
1[a]		1	0.563	0.453	1	0.004	1818.8	10.75
2	Human impacts -> H_2'	2	1.267	0.531	1	0.005	1816.6	8.53
3	Human impacts -> H_2' Human impacts -> Chemodiversity	4	2.924	0.571	1	0.017	1812.5	4.46
4	Human impacts -> H_2' Human impacts -> Chemodiversity Human impacts -> Biodiversity	5	4.335	0.502	1	0.017	1811.2	3.08
5	Human impacts -> H_2' Human impacts -> Chemodiversity Human impacts -> Biodiversity Human impacts -> Energy	6	6.201	0.401	1	0.017	1810.3	2.19
6	Human impacts -> H_2' Human impacts -> Chemodiversity Human impacts -> Biodiversity Human impacts -> Energy Nutrient -> DOM traits	7	8.631	0.280	1	0.018	1810.0	1.92
7	Human impacts -> H_2' Human impacts -> Chemodiversity Human impacts -> Biodiversity Human impacts -> Energy Nutrient -> DOM traits Biodiversity -> DOM traits	8	10.579	0.227	1	0.020	1809.3	1.20
8[b]	Human impacts -> H_2' Human impacts -> Chemodiversity Human impacts -> Biodiversity Human impacts -> Energy Nutrient -> DOM traits Biodiversity -> DOM traits Climate change -> DOM traits	7	6.714	0.459	1	0.018	1808.1	0
China; Positive								
1[a]		1	0.760	0.383	1	0.004	1966.3	15.04

2	Nutrient -> Biodiversity	2	0.768	0.681	1	0.004	1963.4	12.11
3	Nutrient -> Biodiversity Energy -> H_2'	3	0.869	0.833	1	0.004	1960.6	9.33
4	Nutrient -> Biodiversity Energy -> H_2' Human impacts -> H_2'	4	1.086	0.896	1	0.005	1958.0	6.71
5	Nutrient -> Biodiversity Energy -> H_2' Human impacts -> H_2' Nutrient -> DOM traits	5	1.477	0.916	1	0.006	1955.6	4.31
6	Nutrient -> Biodiversity Energy -> H_2' Human impacts -> H_2' Nutrient -> DOM traits Human impacts -> Biodiversity	6	2.526	0.866	1	0.009	1953.9	2.61
7	Nutrient -> Biodiversity Energy -> H_2' Human impacts -> H_2' Nutrient -> DOM traits Human impacts -> Biodiversity Climate change -> H_2'	7	3.888	0.793	1	0.010	1952.6	1.26
8[b]	Nutrient -> Biodiversity Energy -> H_2' Human impacts -> H_2' Nutrient -> DOM traits Human impacts -> Biodiversity Climate change -> H_2' Climate change -> Chemodiversity	8	5.291	0.726	1	0.013	1951.3	0
9	Nutrient -> Biodiversity Energy -> H_2' Human impacts -> H_2' Nutrient -> DOM traits Human impacts -> Biodiversity Climate change -> H_2' Climate change -> Chemodiversity Human impacts -> DOM traits	9	8.220	0.512	1	0.019	1951.6	0.30
10	Nutrient -> Biodiversity Energy -> H_2' Human impacts -> H_2' Nutrient -> DOM traits Human impacts -> Biodiversity Climate change -> H_2' Climate change -> Chemodiversity Human impacts -> DOM traits Nutrient -> H_2'	10	11.134	0.347	1	0.023	1951.9	0.63
Norway; Negative								
1[a]		0	0	0	1	0	1225.2	11.51
2	Energy -> Chemodiversity	1	0.120	0.729	1	0.004	1222.6	8.96

3	Energy -> Chemodiversity Climate change -> Energy	2	0.263	0.877	1	0.006	1220.1	6.48
4	Energy -> Chemodiversity Climate change -> Energy Energy -> H_2'	3	0.656	0.884	1	0.007	1218.0	4.29
5	Energy -> Chemodiversity Climate change -> Energy Energy -> H_2' Nutrient -> DOM traits	4	1.097	0.895	1	0.011	1215.8	2.18
6	Energy -> Chemodiversity Climate change -> Energy Energy -> H_2' Nutrient -> DOM traits Climate change -> Nutrient	5	2.097	0.836	1	0.022	1214.3	0.67
7[b]	Energy -> Chemodiversity Climate change -> Energy Energy -> H_2' Nutrient -> DOM traits Climate change -> Nutrient Climate change -> H_2'	6	3.893	0.691	1	0.024	1213.7	0
8	Energy -> Chemodiversity Climate change -> Energy Energy -> H_2' Nutrient -> DOM traits Climate change -> Nutrient Climate change -> H_2' Chemodiversity -> DOM traits	7	6.735	0.457	1	0.038	1214.1	0.41
Norway; Positive								
1[a]		0	0	0	1	0	1751.2	19.79
2	Human impacts -> Chemodiversity	1	0.097	0.756	1	0.002	1748.3	16.91
3	Human impacts -> Chemodiversity Biodiversity -> DOM traits	2	0.225	0.894	1	0.002	1745.5	14.11
4	Human impacts -> Chemodiversity Biodiversity -> DOM traits Energy -> DOM traits	3	0.391	0.942	1	0.003	1742.8	11.39
5	Human impacts -> Chemodiversity Biodiversity -> DOM traits Energy -> DOM traits Energy -> H_2'	4	0.802	0.938	1	0.006	1740.4	8.97
6	Human impacts -> Chemodiversity Biodiversity -> DOM traits Energy -> DOM traits Energy -> H_2' Climate change -> H_2'	5	1.286	0.936	1	0.008	1738.0	6.66

7	Human impacts -> Chemodiversity Biodiversity -> DOM traits Energy -> DOM traits Energy -> H_2' Climate change -> H_2' Human impacts -> Biodiversity	6	1.892	0.929	1	0.009	1735.9	4.51
8	Human impacts -> Chemodiversity Biodiversity -> DOM traits Energy -> DOM traits Energy -> H_2' Climate change -> H_2' Human impacts -> Biodiversity Nutrient -> Energy	7	2.513	0.926	1	0.011	1733.8	2.43
9	Human impacts -> Chemodiversity Biodiversity -> DOM traits Energy -> DOM traits Energy -> H_2' Climate change -> H_2' Human impacts -> Biodiversity Nutrient -> Energy Chemodiversity -> H_2'	8	3.949	0.862	1	0.012	1732.6	1.2
10[b]	Human impacts -> Chemodiversity Biodiversity -> DOM traits Energy -> DOM traits Energy -> H_2' Climate change -> H_2' Human impacts -> Biodiversity Nutrient -> Energy Chemodiversity -> H_2' Nutrient -> H_2'	9	5.377	0.800	1	0.013	1731.4	0
11	Human impacts -> Chemodiversity Biodiversity -> DOM traits Energy -> DOM traits Energy -> H_2' Climate change -> H_2' Human impacts -> Biodiversity Nutrient -> Energy Chemodiversity -> H_2' Nutrient -> H_2' Human impacts -> DOM traits	10	8.458	0.584	1	0.017	1731.9	0.5

[a] Full SEM models; [b] Best-fitting models shown in red.

Table S5. The hypothesized causal relationships and path coefficients in the structural equation model (Fig. 6a).

Relationship	Path coefficients
Climate change -> Nutrient	$\lambda_{nut,temp}$
Human impacts -> Nutrient	$\lambda_{nut,N}$
Climate change -> Energy	$\lambda_{energy,temp}$
Human impacts -> Energy	$\lambda_{energy,N}$
Nutrient -> Energy	$\lambda_{energy,nut}$
Climate change -> Biodiversity	$\lambda_{biodiv,temp}$
Human impacts -> Biodiversity	$\lambda_{biodiv,N}$
Nutrient -> Biodiversity	$\lambda_{biodiv,nut}$
Energy -> Biodiversity	$\lambda_{biodiv,energy}$
Climate change -> Chemodiversity	$\lambda_{chemodiv,temp}$
Human impacts -> Chemodiversity	$\lambda_{chemodiv,N}$
Nutrient -> Chemodiversity	$\lambda_{chemodiv,nut}$
Energy -> Chemodiversity	$\lambda_{chemodiv,energy}$
Climate change -> DOM traits	$\lambda_{trait,temp}$
Human impacts -> DOM traits	$\lambda_{trait,N}$
Nutrient -> DOM traits	$\lambda_{trait,nut}$
Energy -> DOM traits	$\lambda_{trait,energy}$
Biodiversity -> DOM traits	$\lambda_{trait,biodiv}$
Chemodiversity -> DOM traits	$\lambda_{trait,chemodiv}$
Climate change -> H_2'	$\lambda_{H2,temp}$
Human impacts -> H_2'	$\lambda_{H2,N}$
Nutrient -> H_2'	$\lambda_{H2,nut}$
Energy -> H_2'	$\lambda_{H2,energy}$
Biodiversity -> H_2'	$\lambda_{H2,biodiv}$
Chemodiversity -> H_2'	$\lambda_{H2,chemodiv}$
DOM traits -> H_2'	$\lambda_{H2,trait}$

Supplementary Figures

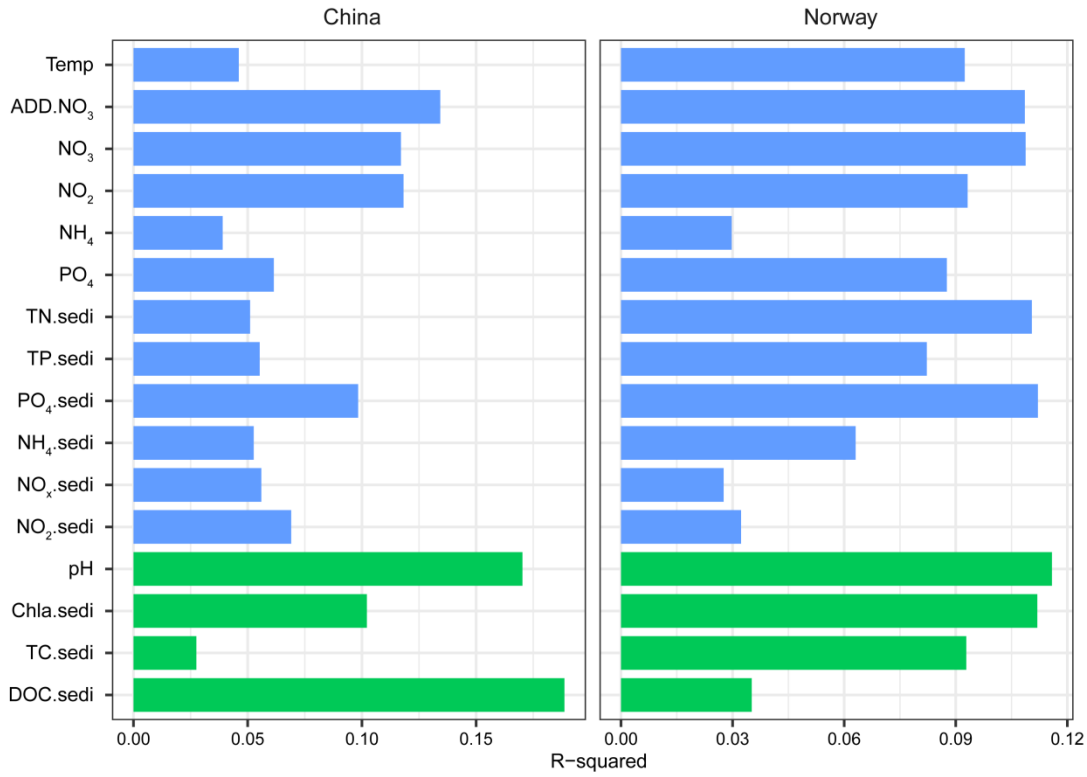

Figure S1. Bar plots showing R-squared to identify the effects of environmental (blue) and energy supply (green) variables on molecular composition of DOM in China and Norway. R-squared was determined by permutational multivariate analysis of variance (PERMANOVA) with 999 permutations and was statistically significant ($P \leq 0.001$) for explanatory variables. R-squared for each explanatory variable stands for the explained variations in the differences of DOM molecular composition among the samples. Nitrate addition ($ADD.NO_3$) was used to represent nutrient enrichment as the ratio between nitrate and phosphorus in the initial overlying water was constant. The abbreviations of explanatory variables are detailed in Table S2.

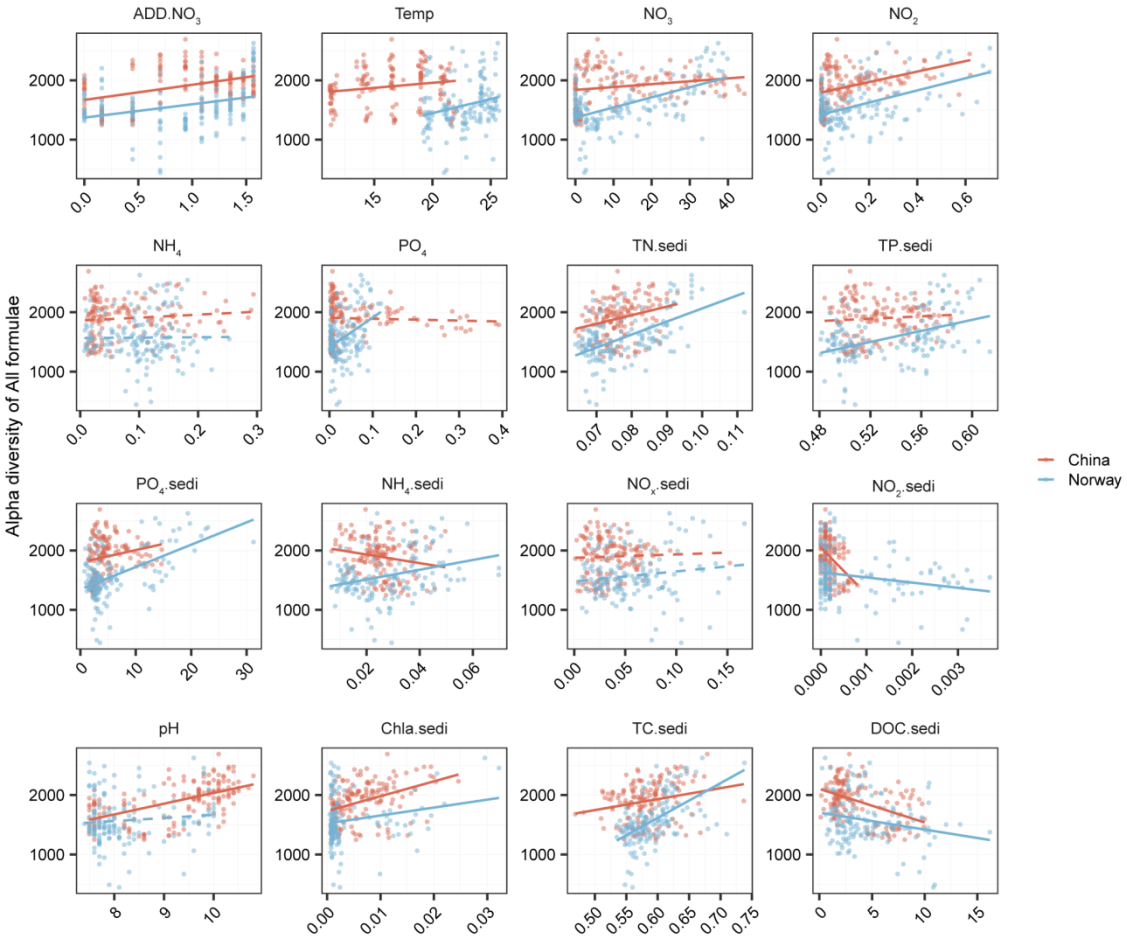

143

144 **Figure S2**. The relationships between DOM alpha diversity (i.e., molecular richness) and
145 explanatory variables in China (red lines) and Norway (blue lines). We plotted alpha
146 diversity against the variables relevant to environment and energy supply (Table S2). The
147 relationships are indicated by solid ($P \leq 0.05$) and dotted ($P > 0.05$) lines estimated using
148 linear models with one-sided F-statistics.

149

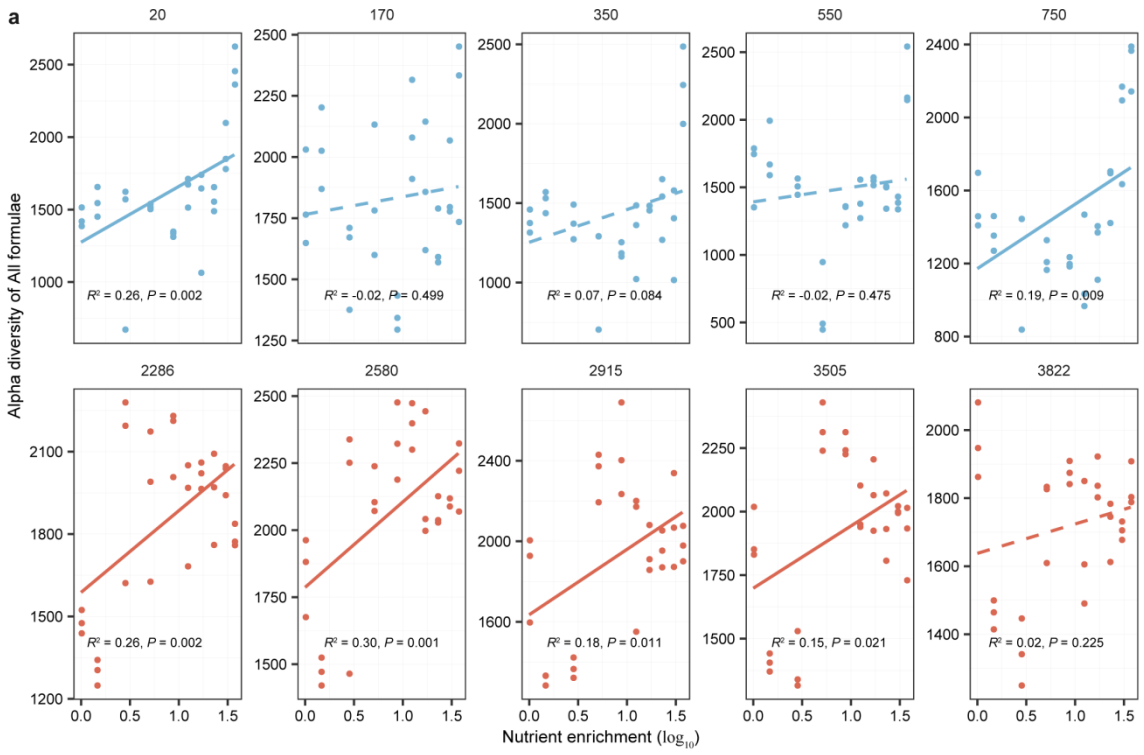

150

151 **Figure S3**. The relationships between nutrient enrichment and DOM alpha diversity or
152 molecular traits in China (red lines) and Norway (blue lines) at different elevations (20 to
153 3,822 m a.s.l.). We considered richness for all formulae (a) and also molecular traits such
154 as weighted means of mass (b), H/C ratio (c), O/C ratio (d) and AI_{Mod} (e) in China (red
155 lines and dots) and Norway (blue lines and dots). We used nitrate addition to represent
156 nutrient enrichment as the ratio between nitrate and phosphorus in the initial overlying
157 water was constant. We plotted the richness or traits against the nutrient gradient of
158 nitrate, and their relationships are indicated by solid ($P \leq 0.05$) and dotted ($P > 0.05$) lines
159 using linear models with one-sided F-statistics.

160

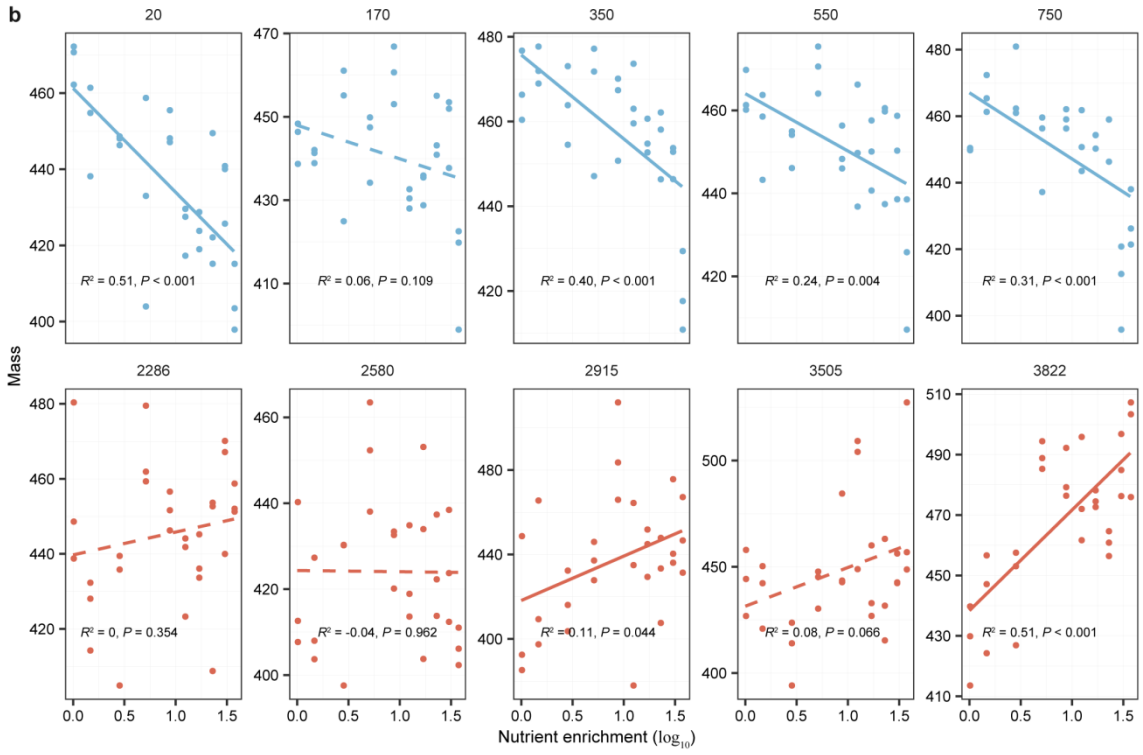

161

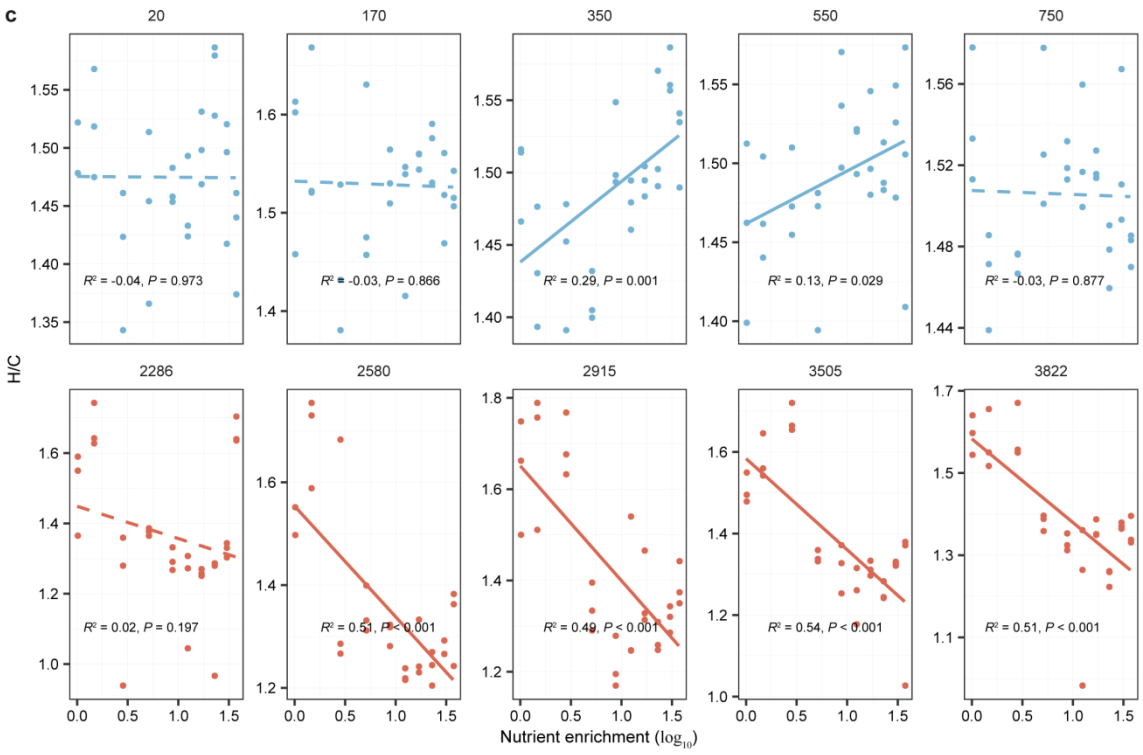

162

163 **Figure S3**. Continued. Weighted means of mass (b), and H/C ratio (c).

164

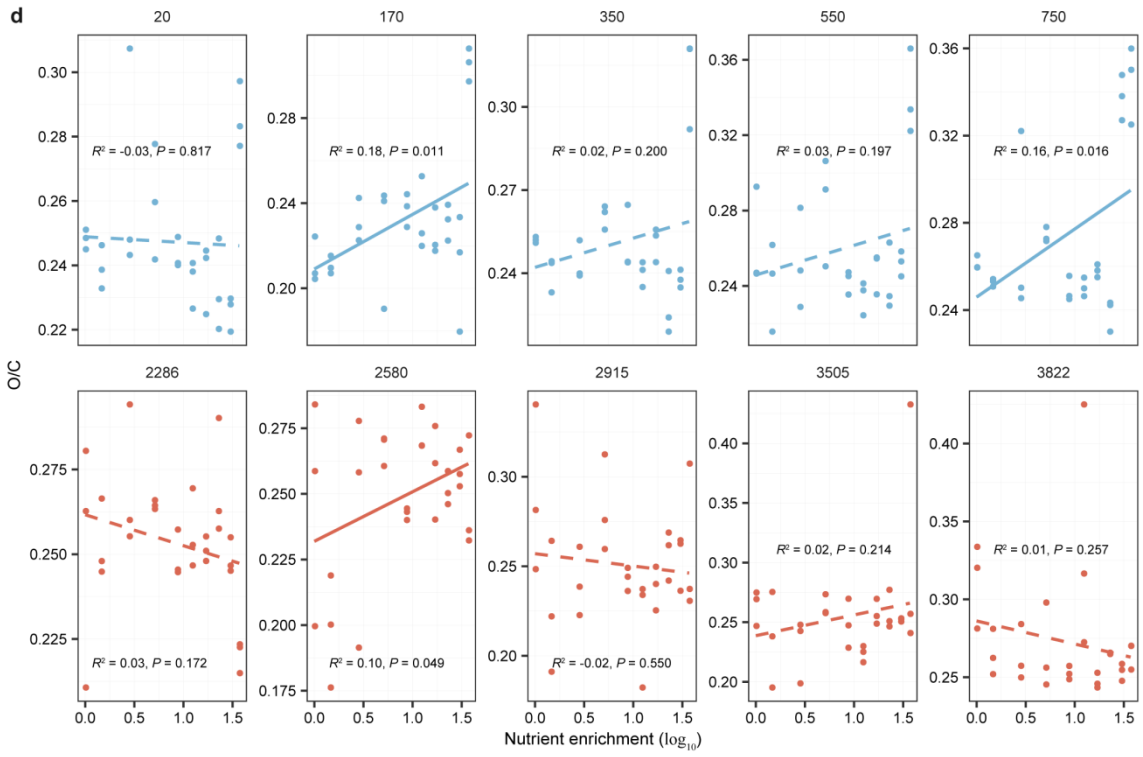

165

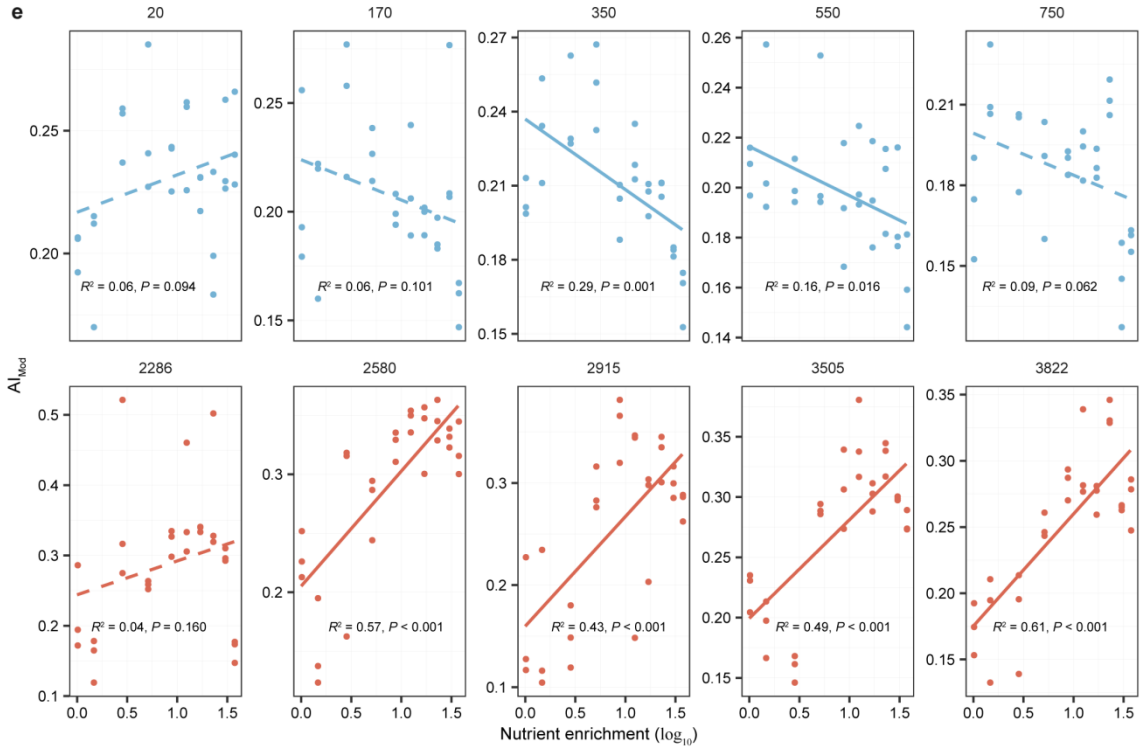

166

167 **Figure S3**. Continued. Weighted means of O/C ratio (d) and AI_{Mod} (e).

168

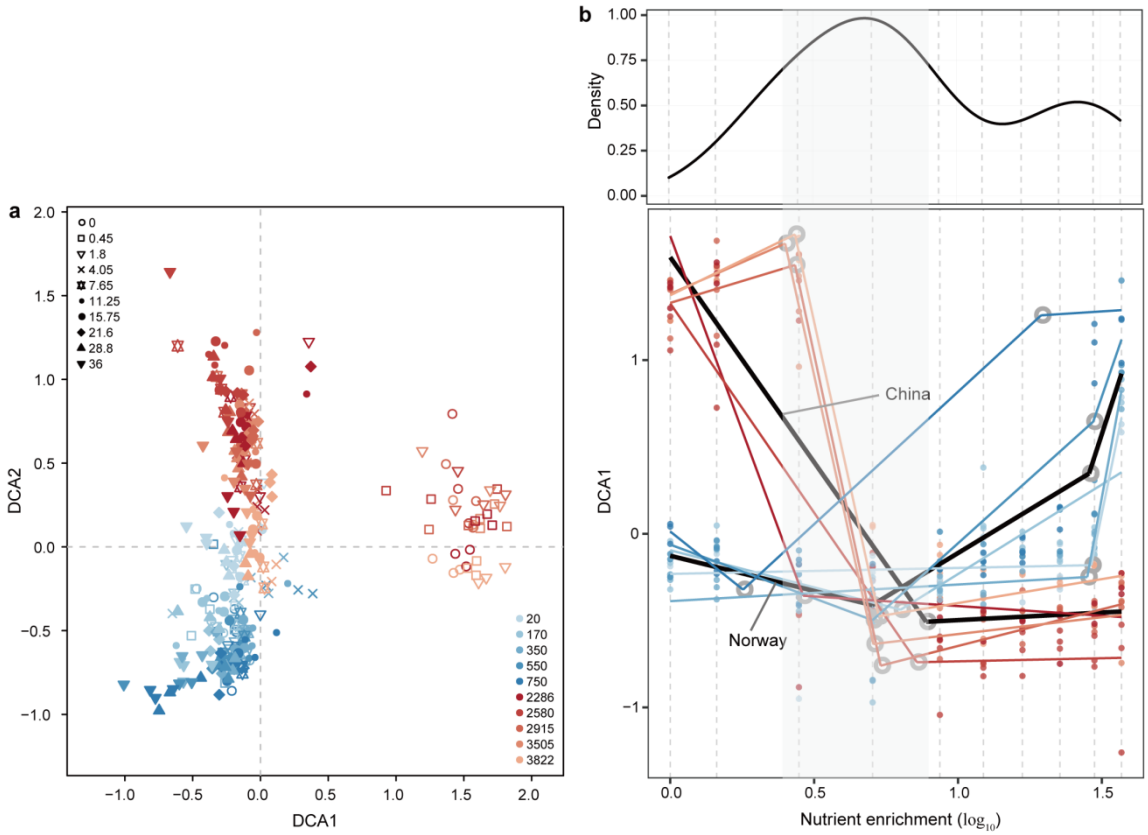

Figure S4. Variations in DOM compositions along the nutrient gradient of nitrate. (a) Detrended correspondence analyses (DCA) of DOM compositions. (b) Nutrient breakpoint estimation of the first axis of the DCA of DOM composition for each elevation using piecewise regression analysis with Bayesian Information Criteria statistics (Muggeo, 2008). The upper panel is a density plot of the distribution of breakpoints. The black thick lines in the lower panel indicate each region (i.e., China and Norway), and the colored dots or lines indicate the elevations of the two regions, which are consistent with the figure legend of Fig. S4a. The gray open circles indicate nutrient breakpoints. The vertical gray lines indicate the ten experimental nutrient levels. We found that, along the nutrient gradient, there were breakpoints of the first axis of the DCA mostly occurring between 1.80 and 4.05 mg N L^{-1} (indicated by gray shade) especially in China.

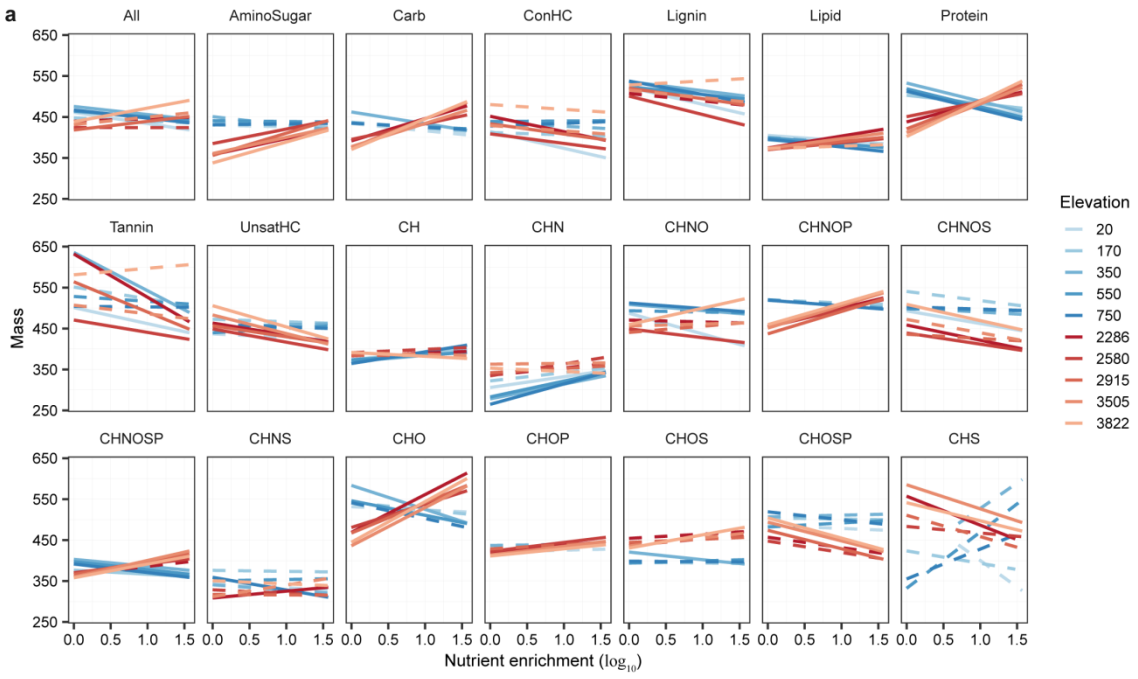

183

184 **Figure S5**. Effects of nutrient enrichment on DOM traits for all formulae and subsets of
185 formulae within compound classes or elemental combinations across different elevations
186 in China (red lines) and Norway (blue lines). We considered molecular traits such as
187 weighted means of mass (a), H/C ratio (b) and AI_{Mod} (c), which were plotted against the
188 nutrient gradient of nitrate, and their relationships are indicated by the solid ($P \leq 0.05$) or
189 dotted ($P > 0.05$) lines using linear models with one-sided F-statistics. The details of
190 abbreviations of DOM traits are available in Table S1. We found that nutrient enrichment
191 increased the weighted means of molecular mass more strongly at higher elevations in
192 China (with maximal 495 Da at 3,822 m a.s.l.), but decreased more strongly at lower
193 elevations in Norway (with minimal 405 Da at 20 m a.s.l.). This finding implies that
194 nutrient enrichment leads to an increase in the molecular mass especially at colder
195 temperatures in subtropical regions, but a decline at the warmer temperatures in subarctic
196 regions.

197

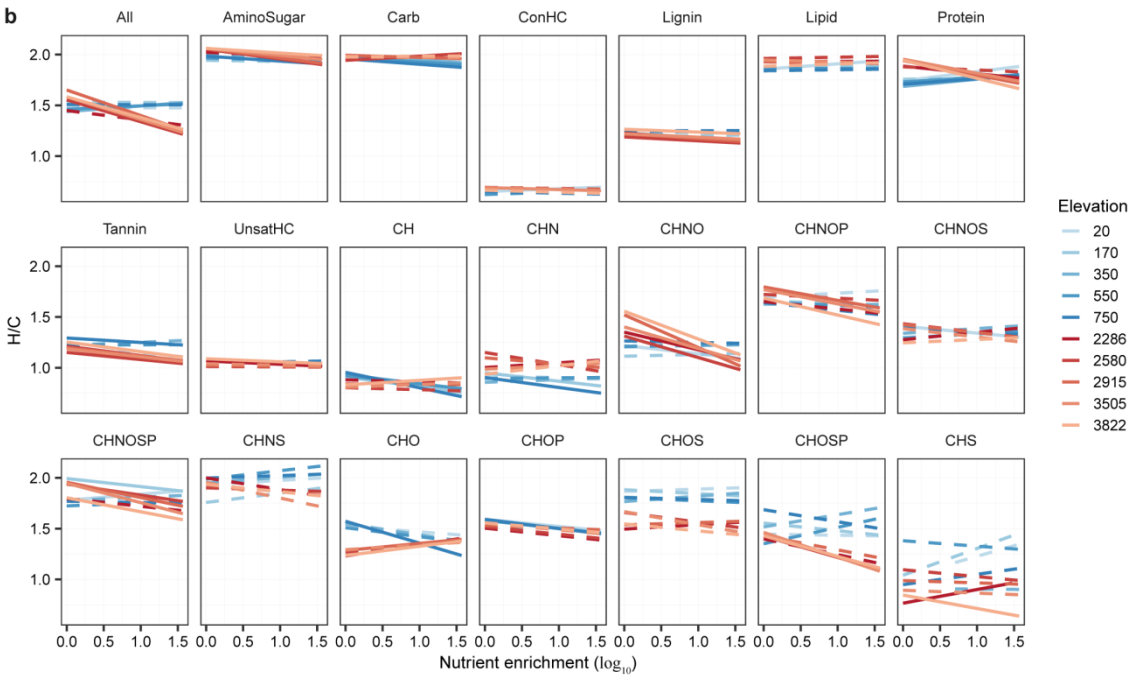

198

199 **Figure S5**. Continued. Weighted means of H/C ratio (b).

200

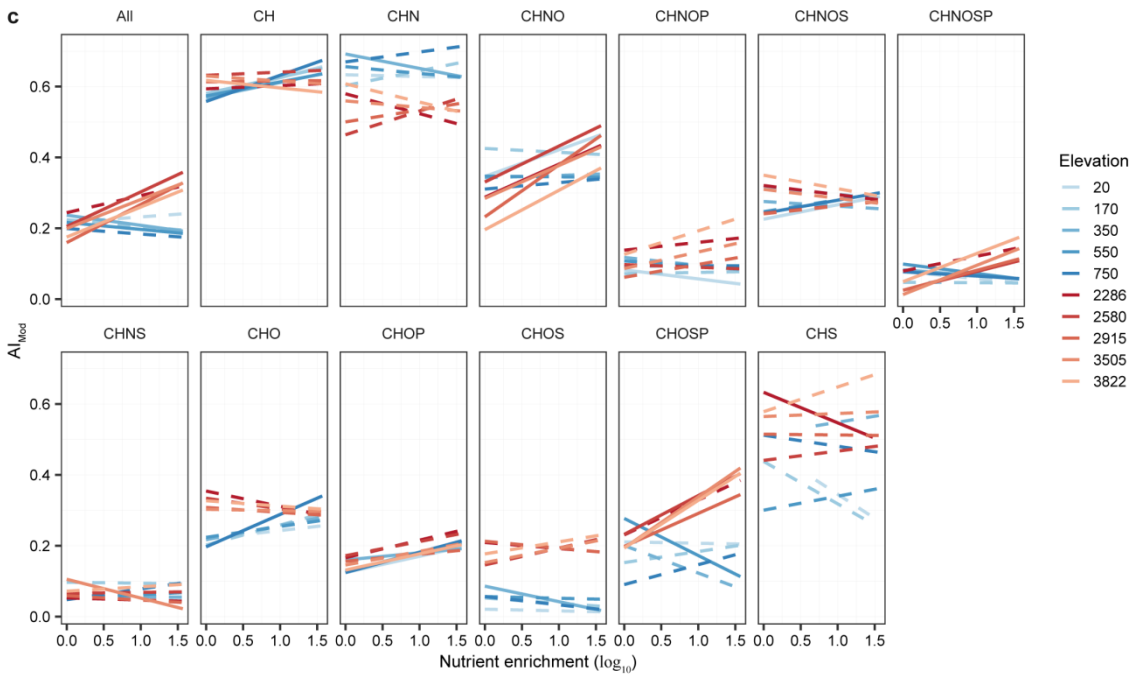

201

202 **Figure S5**. Continued. Weighted means of AI_{Mod} (c).

203

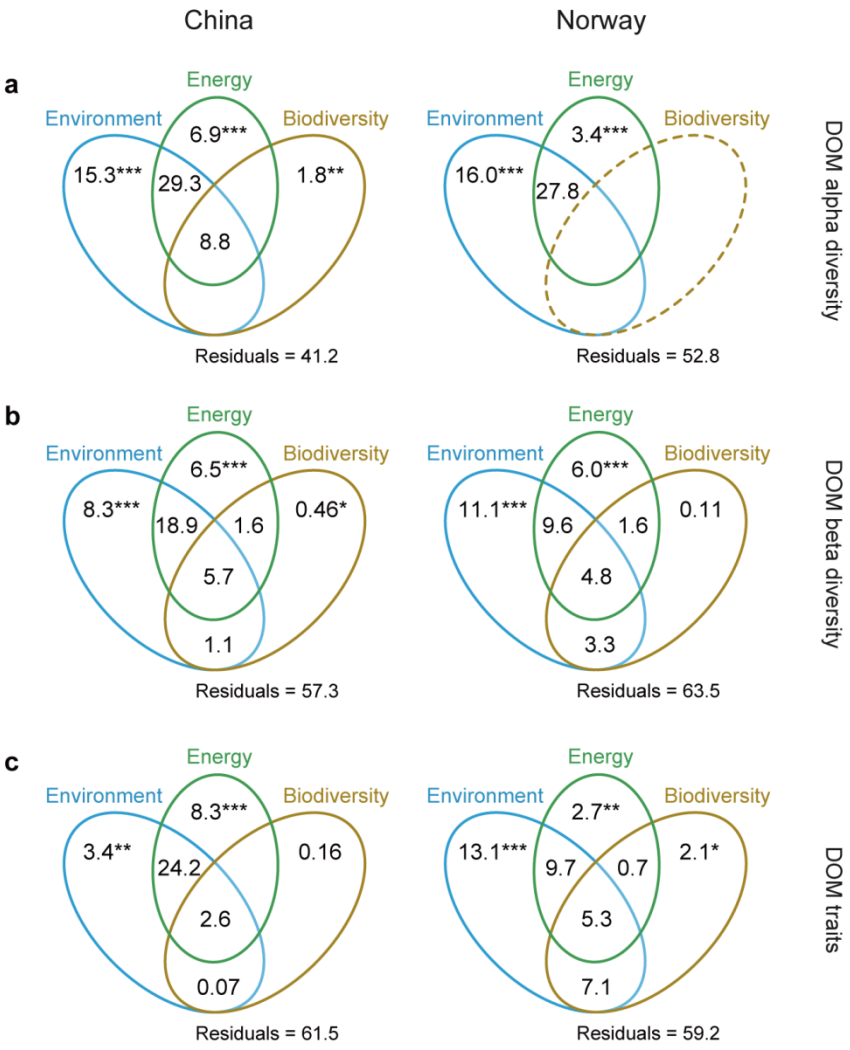

204

205 **Figure S6**. The roles of microbes in explaining the alpha diversity (upper panel), beta
206 diversity (middle panel) and molecular traits (lower panel) of DOM using variation
207 partitioning analysis. The numbers indicate the variance explained (%) by environments,
208 energy supply and bacterial biodiversity which were described in detail in Table S2. The
209 significance was examined using one-sided F-statistics and asterisks represent statistically
210 significant effects at ***, $P \leq 0.001$; **, $P \leq 0.01$; *, $P \leq 0.05$.

211

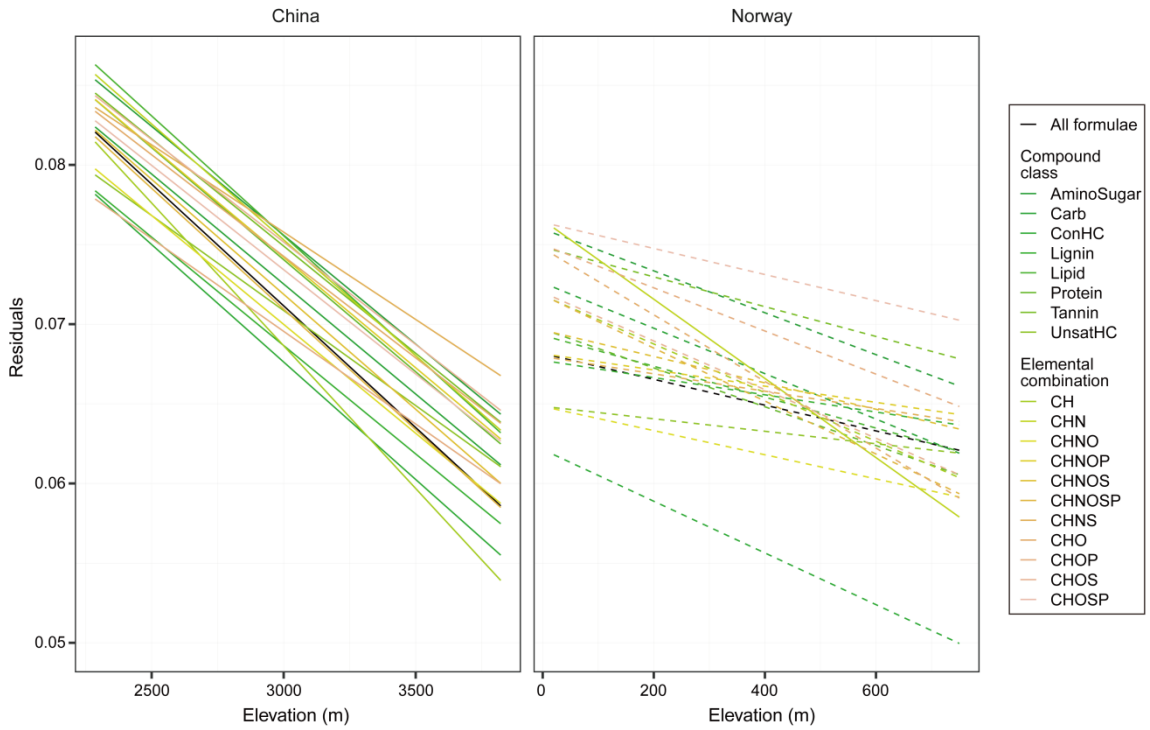

212

213 **Figure S7**. The effects of elevation on DOM-microbe associations indicated by
214 Procrustes residuals, that is, the difference in composition between DOM and bacteria for
215 each microcosm. These effects are indicated by solid ($P \leq 0.05$) or dotted ($P > 0.05$) lines
216 estimated using linear models with one-sided F-statistics. The colours of the lines indicate
217 the DOM composition for all formulae and categories of compound classes or elemental
218 combinations.

219

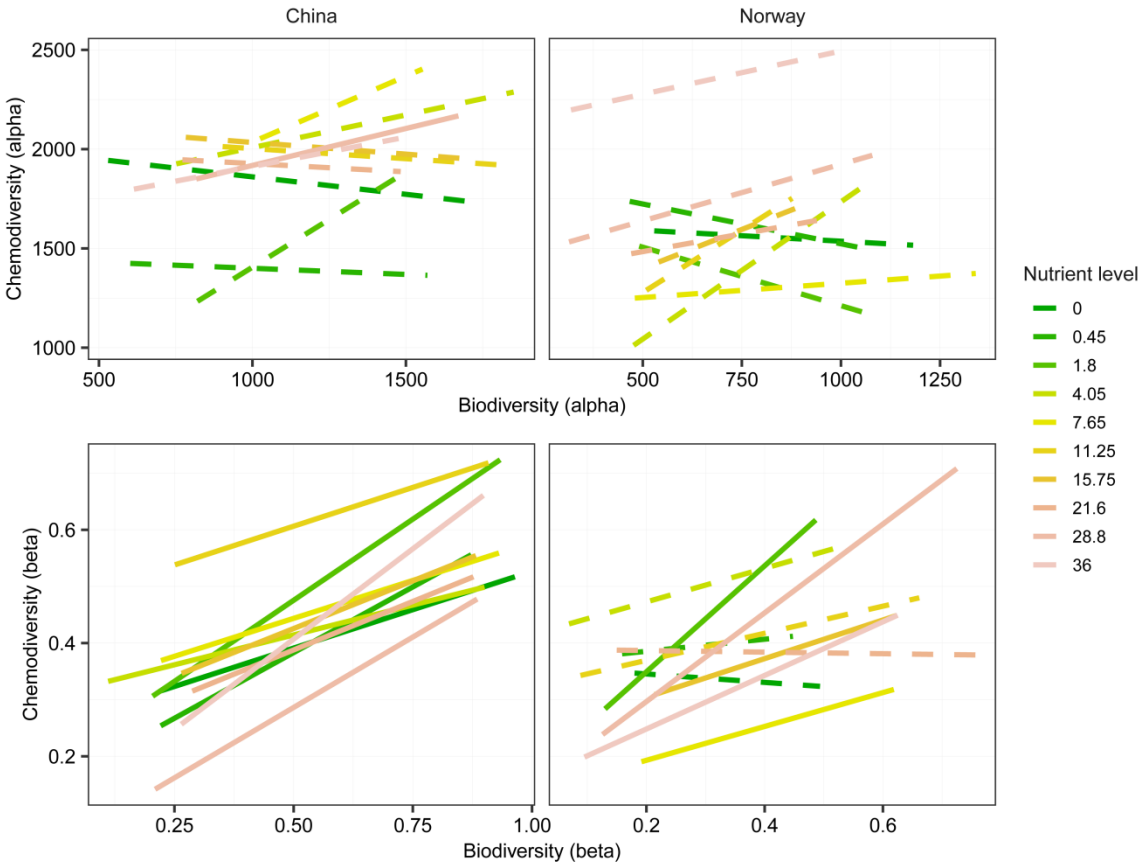

220

221 **Figure S8**. The relationships between chemodiversity and bacterial diversity in China
222 and Norway along the nutrient gradient of nitrate. Upper panel: Alpha diversity (richness)
223 of DOM molecular formulae and bacterial OTUs. Lower panel: Beta diversity determined
224 by the Bray–Curtis dissimilarity index for the mixtures of molecular formulae and the
225 communities of OTUs. Each line visualises the relationship of alpha or beta diversity
226 between DOM and bacteria across 15 samples at each nutrient level in China or Norway.
227 The relationships are indicated by solid ($P \leq 0.05$) and dotted ($P > 0.05$) lines using linear
228 models, and the significance was determined by ANOVA with one-sided F-statistics
229 (upper panels) or two-sided Mantel test with 999 permutations (lower panels).

230

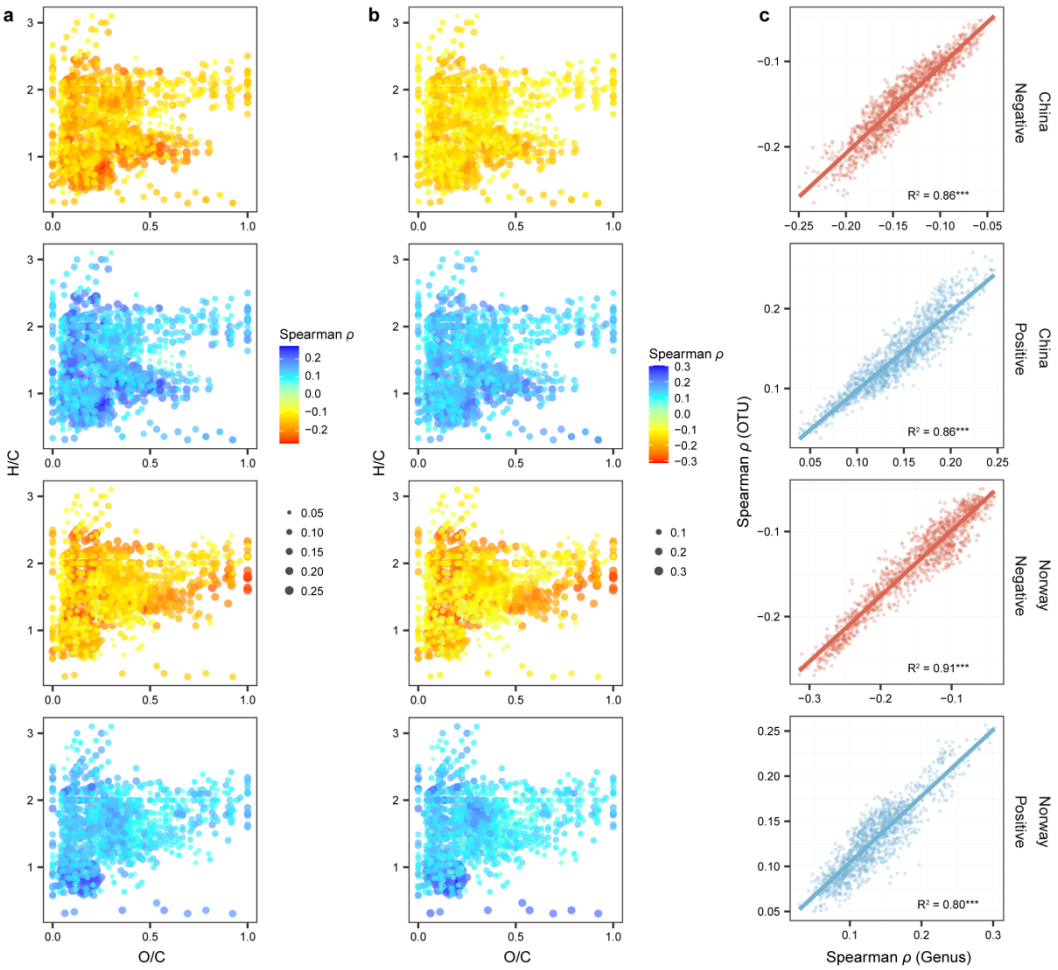

231

232 **Figure S9**. Molecular formulae correlating with bacterial OTUs (a) or genera (b) in
233 China and Norway using Spearman's rank correlation (ρ). Each molecule is colored by
234 the mean ρ value of negative or positive correlations across all bacterial OTUs, and the
235 absolute value of mean ρ is indicated by the dot size. (c) The relationships in Spearman ρ
236 between bacterial OTU and genus levels for both negative and positive correlations in
237 China and Norway. Solid lines indicate significant linear fits with one-sided F-statistics
238 ($P \leq 0.05$).

239

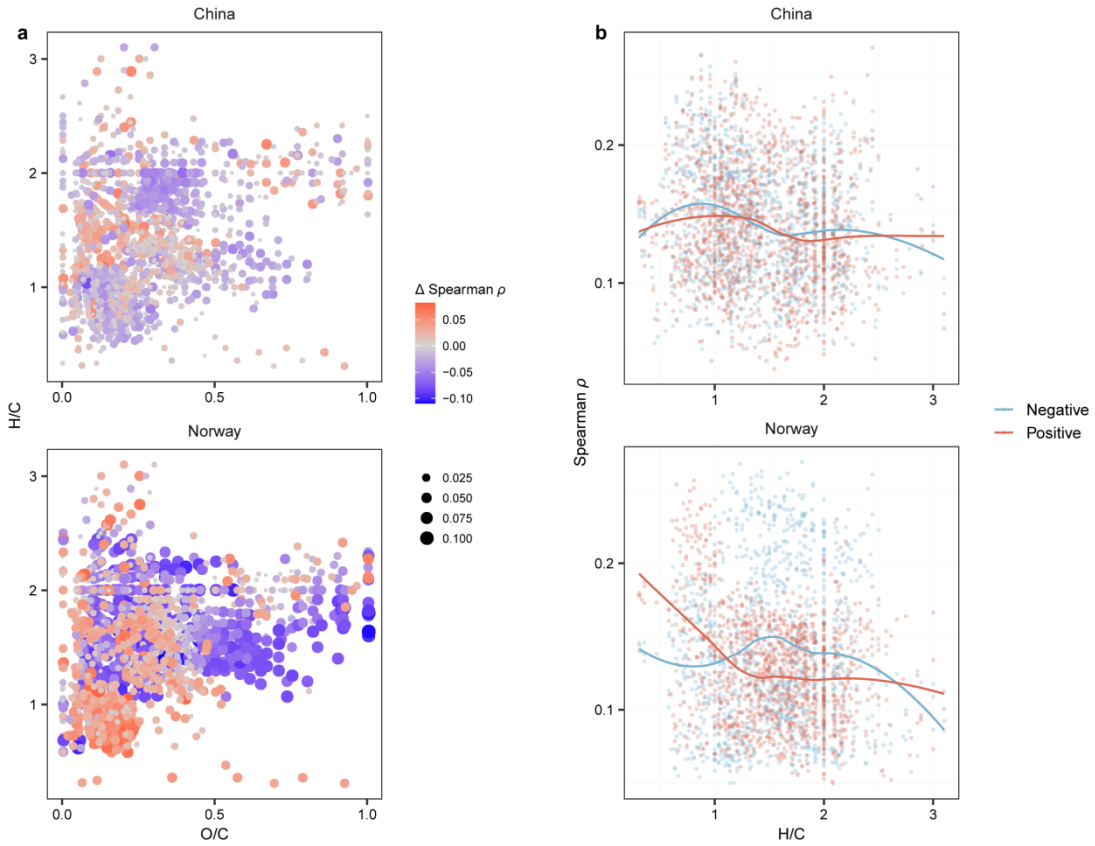

240

241 **Figure S10**. Correlations between DOM and bacteria regarding molecular traits. (a)
242 Molecular formulae correlating with bacterial OTUs in China and Norway using
243 Spearman's rank correlation (ρ). Each molecule is colored by difference in the absolute
244 Spearman ρ ($\Delta\rho$). The difference for each molecule was calculated by subtracting the
245 mean absolute ρ value of the negative correlations across all bacterial OTUs from that of
246 the negative correlations, and the absolute value of ρ difference is indicated by the dot
247 size. (b) The patterns of absolute ρ values of positive and negative correlations along the
248 gradient of H/C ratio visualized with loess regression models.

249

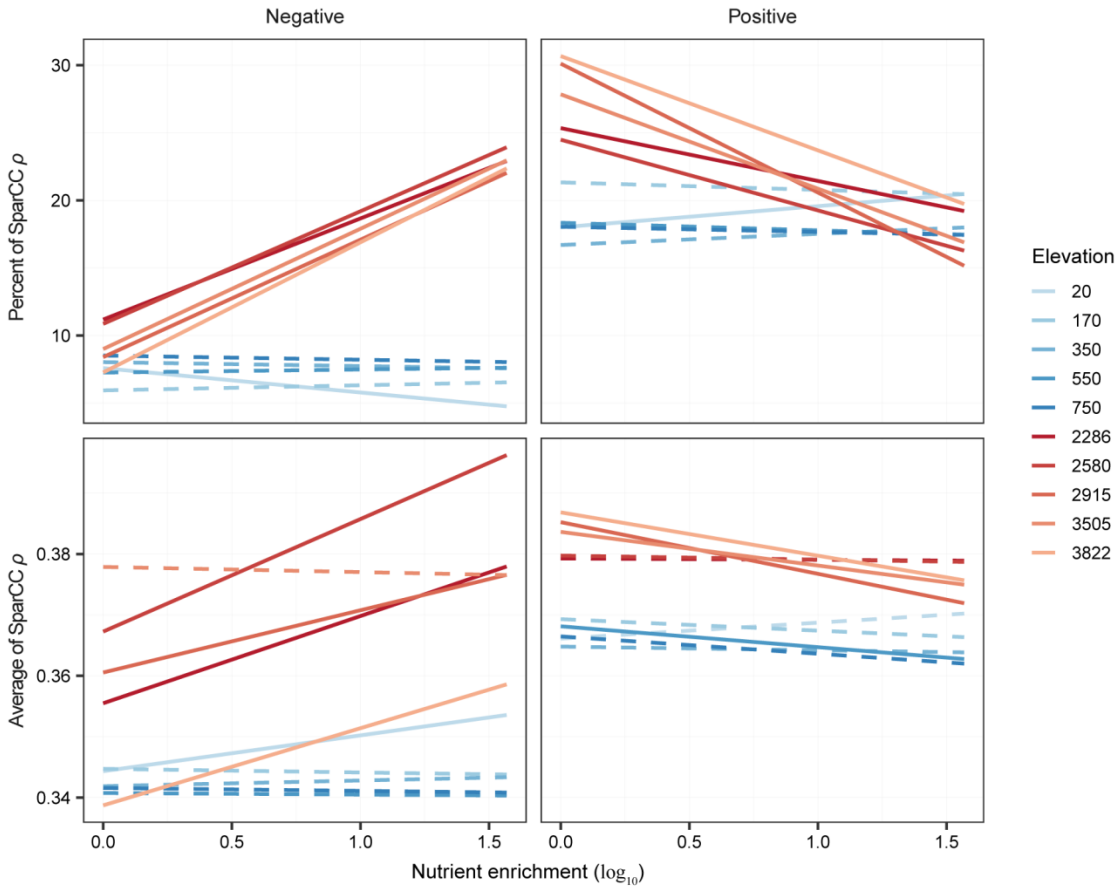

Figure S11. The effects of nutrient enrichment on weighted means of indices of DOM-bacteria bipartite networks. The network indices include the percent and average of strong correlations (|SparCC ρ| $\geq$ 0.3) of negative or positive networks. We plotted these indices against the nutrient gradient of nitrate for both negative (left panel) and positive (right panel) networks for each elevation in China (red lines) or Norway (blue lines), and their relationships are indicated by solid ($P \leq 0.05$) or dotted ($P > 0.05$) lines using linear models with one-sided F-statistics.

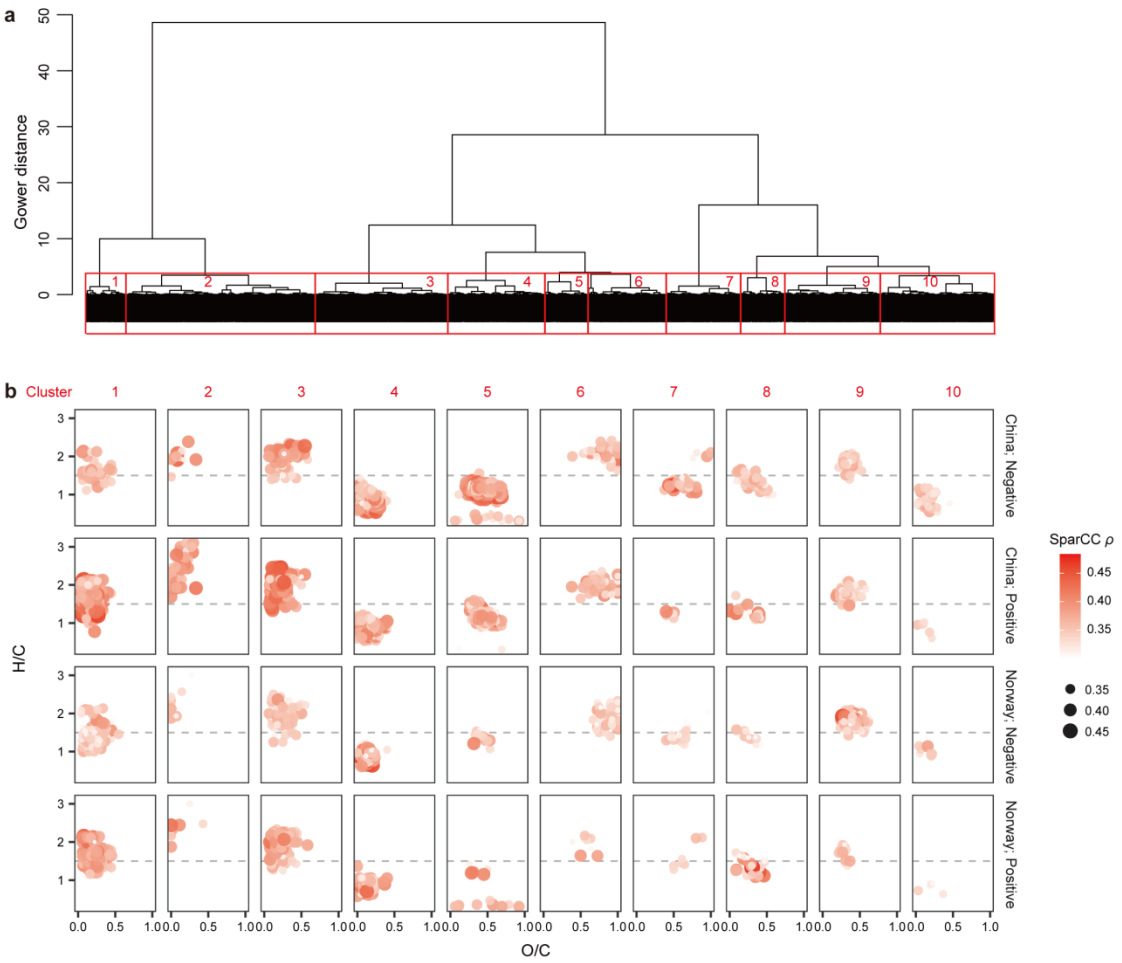

259

260 **Figure S12**. Correlations between DOM and bacteria regarding molecular traits. (a)
261 Cluster analysis identified ten molecular sub-mixtures based on 16 molecular traits (Table
262 S1). (b) Location of the ten clusters in Van Krevelen space with colour- and size-coded
263 correlations between molecule-specific intensities and the relative abundance of bacterial
264 genera using SparCC (Sparse Correlations for Compositional data). For each molecule,
265 we showed the mean absolute SparCC ρ values of negative or positive correlations across
266 all bacterial OTUs. We considered only strong correlations ($|\text{SparCC } \rho| \geq 0.3$).

267

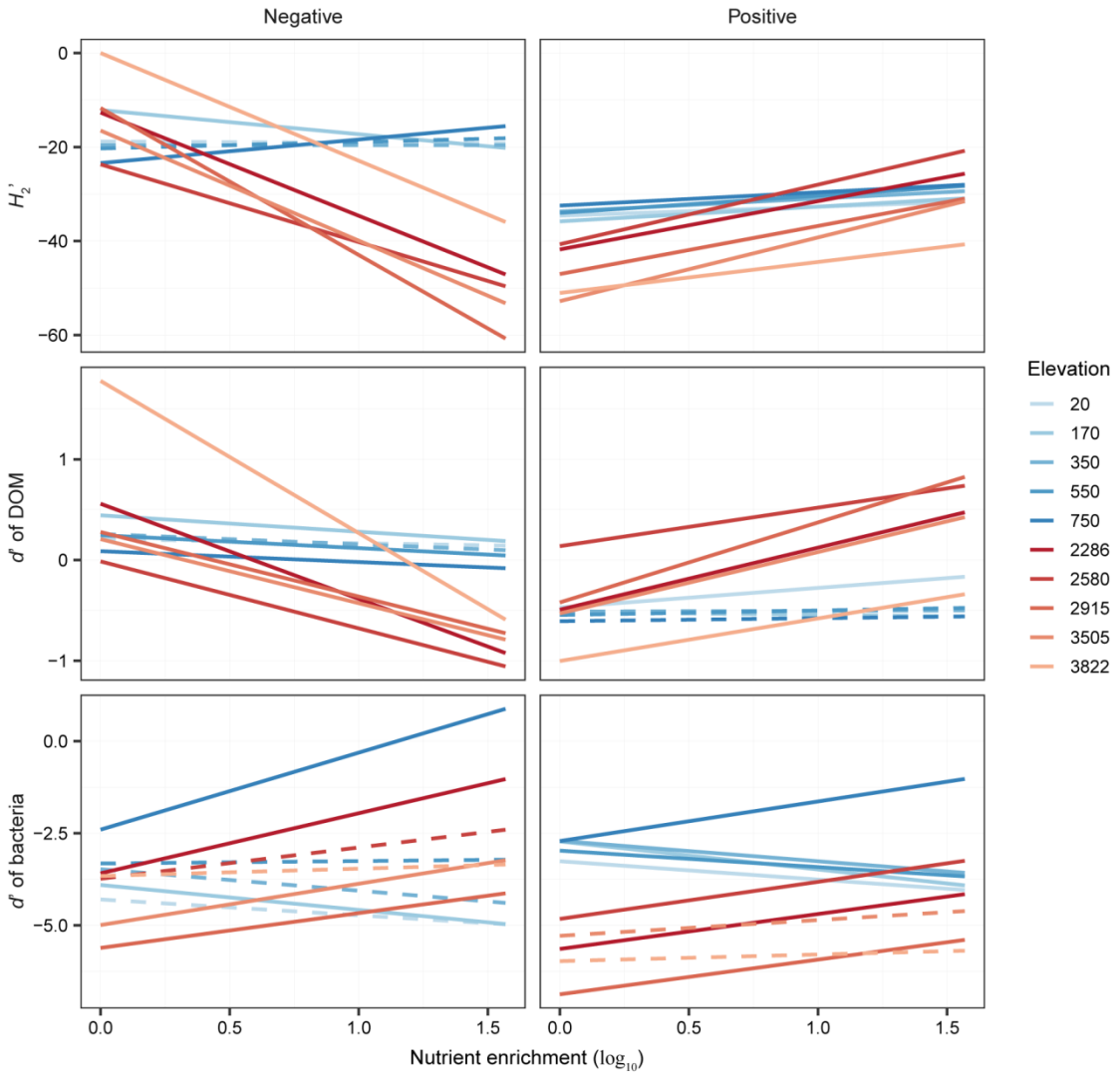

Figure S13. The effects of nutrient enrichment on specialization indices of DOM-bacteria bipartite networks. The specialization indices include network-level specialization H_2', and the weighted means of specialization d' for DOM molecules and bacterial genera. We plotted these indices against the nutrient gradient of nitrate for both negative (left panel) and positive (right panel) networks for each elevation in China (red lines) or Norway (blue lines), and their relationships are indicated by solid ($P \leq 0.05$) or dotted ($P > 0.05$) lines using linear models with one-sided F-statistics.

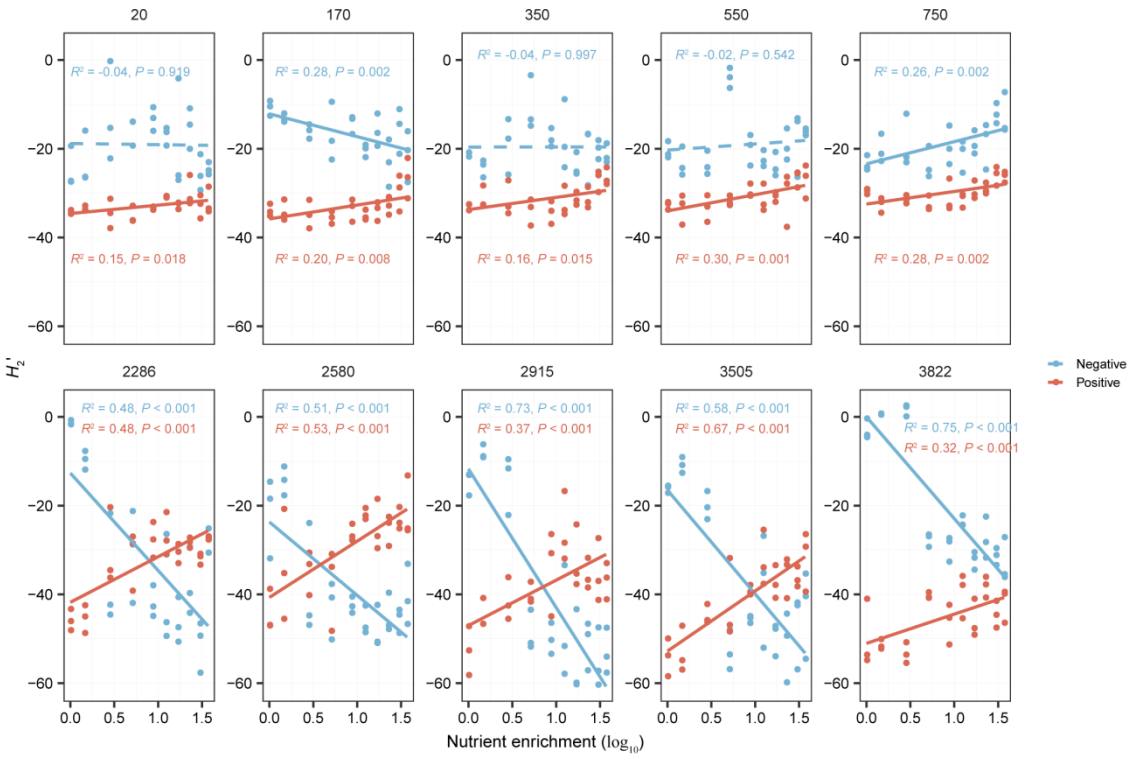

277

278 **Figure S14**. The effect of nutrient enrichment on the specialization H_2' of DOM-bacteria
279 bipartite networks. We plotted the H_2' against the nutrient gradient of nitrate for both
280 negative (blue lines) and positive (red lines) networks for each elevation in China or
281 Norway, and their relationships are indicated by solid ($P \leq 0.05$) or dotted ($P > 0.05$)
282 lines using linear models with one-sided F-statistics.

283

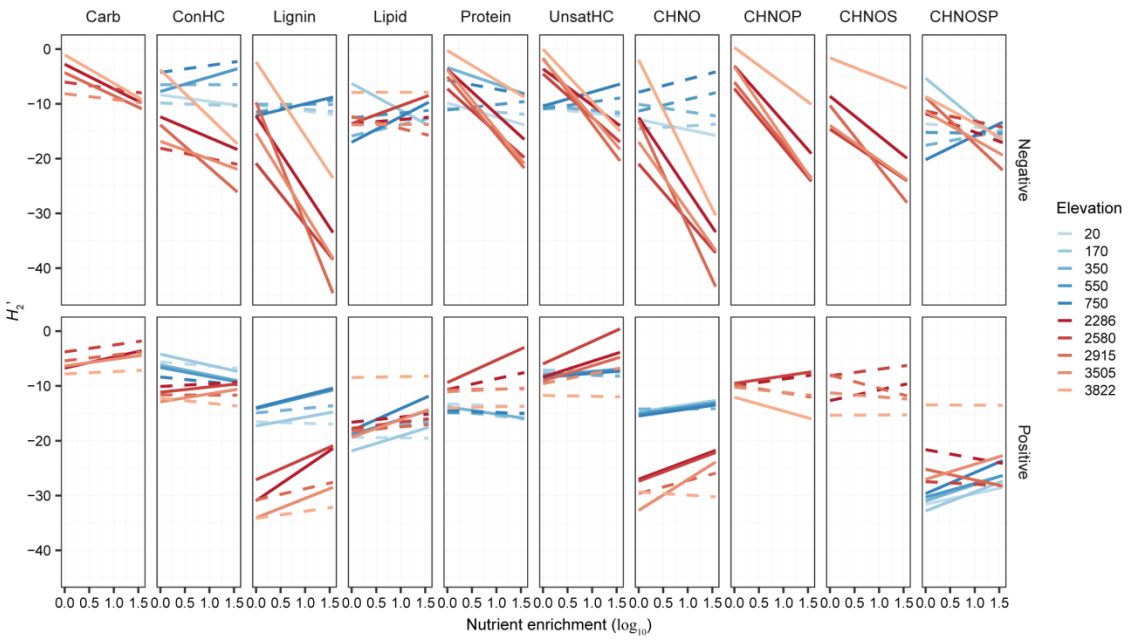

284

285 **Figure S15**. The effects of nutrient enrichment on the specialization H_2' of DOM-
286 bacteria bipartite networks for all formulae and subsets of formulae within the category of
287 compound classes or elemental combinations. We plotted the H_2' against the nutrient
288 gradient of nitrate for both negative (upper panel) and positive (lower panel) networks for
289 each elevation in China (red lines) or Norway (blue lines), and their relationships are
290 indicated by solid ($P \leq 0.05$) or dotted ($P > 0.05$) lines using linear models with one-sided
291 F-statistics.

292

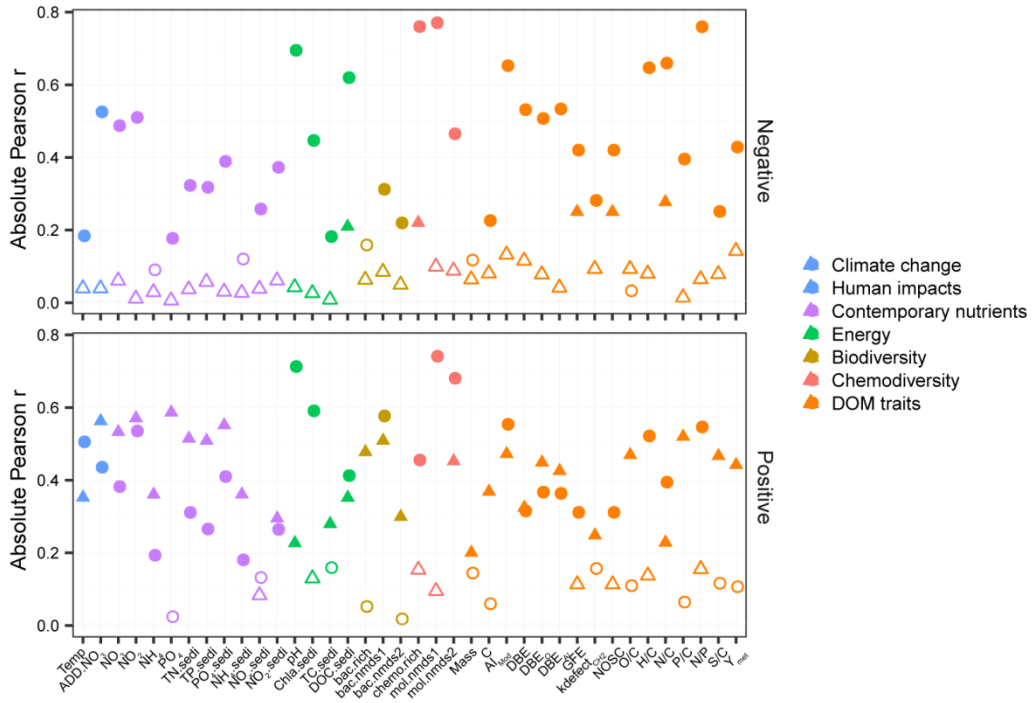

293

294 **Figure S16**. The relative influence of explanatory variables on the specialization H_2' of
295 negative (upper panel) and positive (lower panel) DOM-bacteria bipartite networks using
296 Pearson correlation analysis. Each circle and triangle are the absolute values of Pearson r
297 for individual explanatory variable in China and Norway, respectively. Solid and open
298 circles or triangles indicate the significant ($P \leq 0.05$) and non-significant ($P > 0.05$) two-
299 sided Pearson r, respectively. The details of abbreviations of explanatory variables are
300 available in Table S1.

301

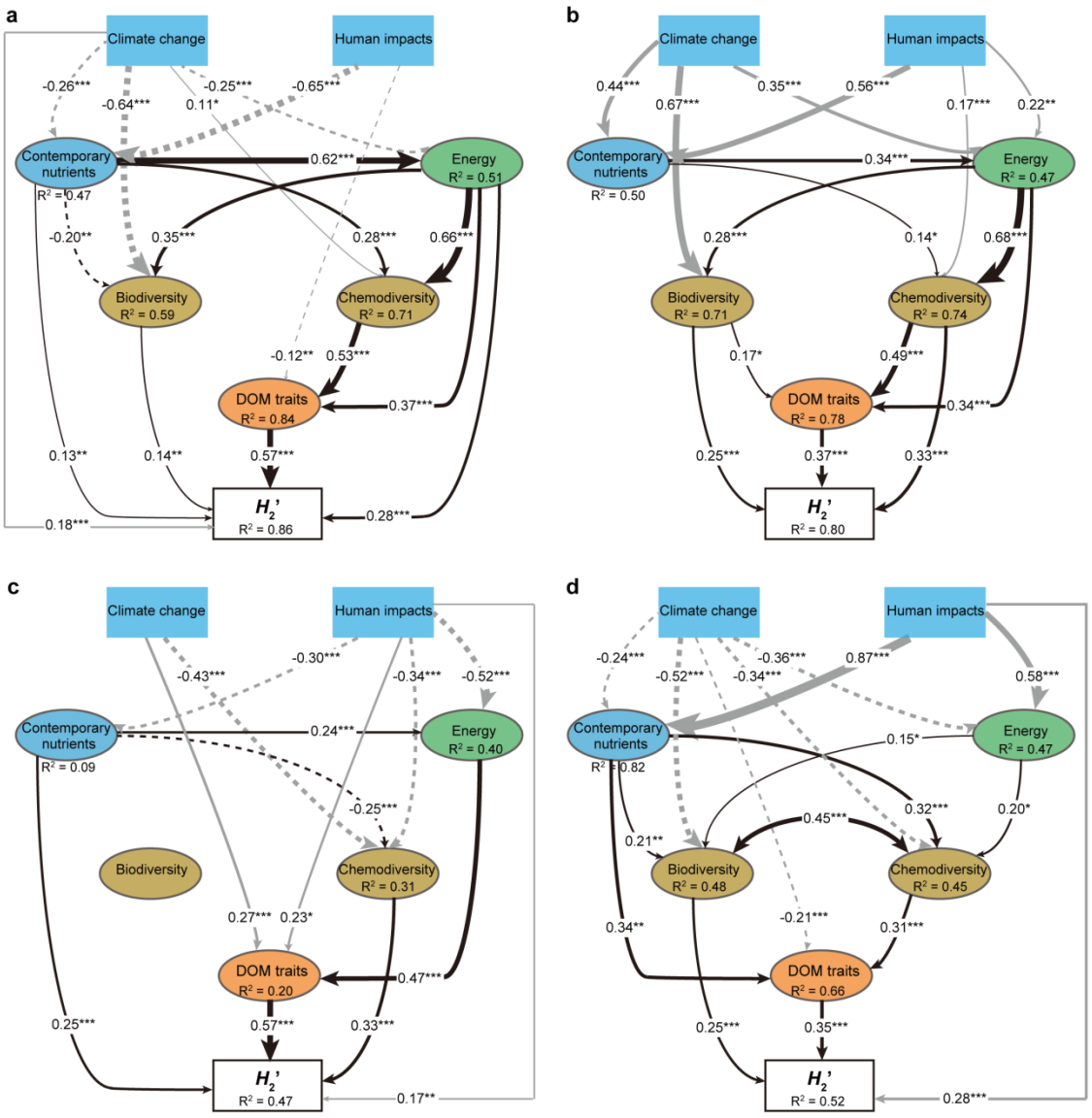

Figure S17. Structural equation models to explain specialization of DOM-bacteria bipartite networks. Best-fitting models illustrate the effects of predictor variables on the H_2' of negative (a, c) and positive (b, d) bipartite networks in China (a-b) or Norway (c-d). Predictor variables were grouped by climate change, human impacts, contemporary nutrients, energy supply, biodiversity, chemodiversity and DOM traits, and described in detail in Table S3. R^2 denotes the proportion of variance explained for the endogenous variables. Dotted and solid arrows indicate the two-sided statistically significantly negative and positive (***, $P \leq 0.001$; **, $P \leq 0.01$; *, $P \leq 0.05$) relationships, respectively, with z-statistics. Grey or black arrows indicate the hypothesized relationships among the

312 exogenous or endogenous variables and H_2', respectively. Arrow widths and
313 accompanying numbers are the relative effects (that is, standardized path coefficients) of
314 modeled relationships. Composite and observed variables are indicated in ovals and
315 rectangles, respectively. Details of model fit are summarized in Table S4.

316

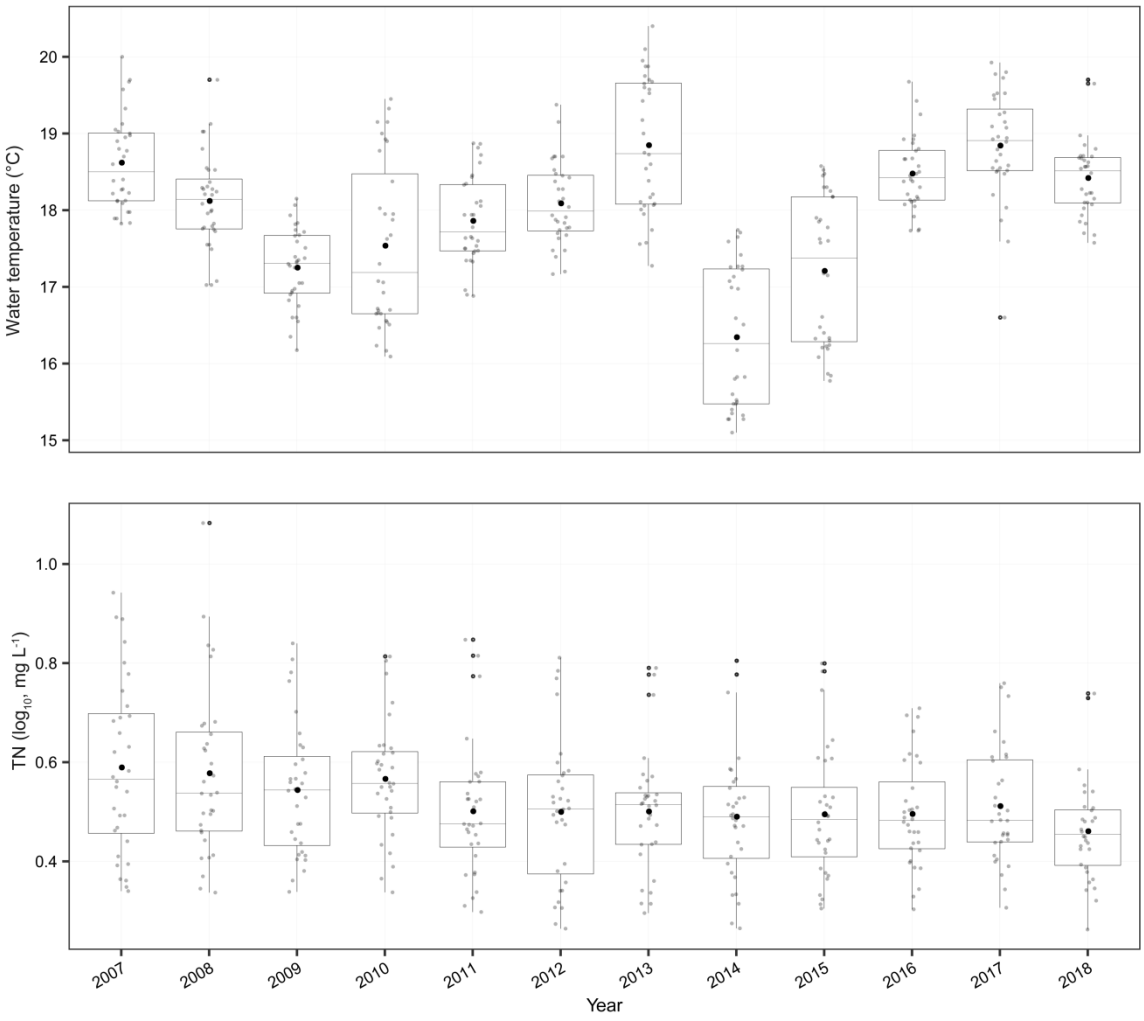

317

318 **Figure S18**. Water temperature and total nitrogen (TN) during 2007-2018 in Taihu Lake.
319 n = 32 sampling sites across the whole of Taihu Lake (Fig. S19a). The grey dots indicate
320 water temperature and TN for individual sites and black dots are the mean values for each
321 year. The boxes extend from 25th to 75th percentile (first and third quartiles), median is
322 marked by the line, and the ends of whiskers indicate the minimum and maximum values
323 within 1.5× the inter-quartile range from the first and third quartiles, respectively.

324

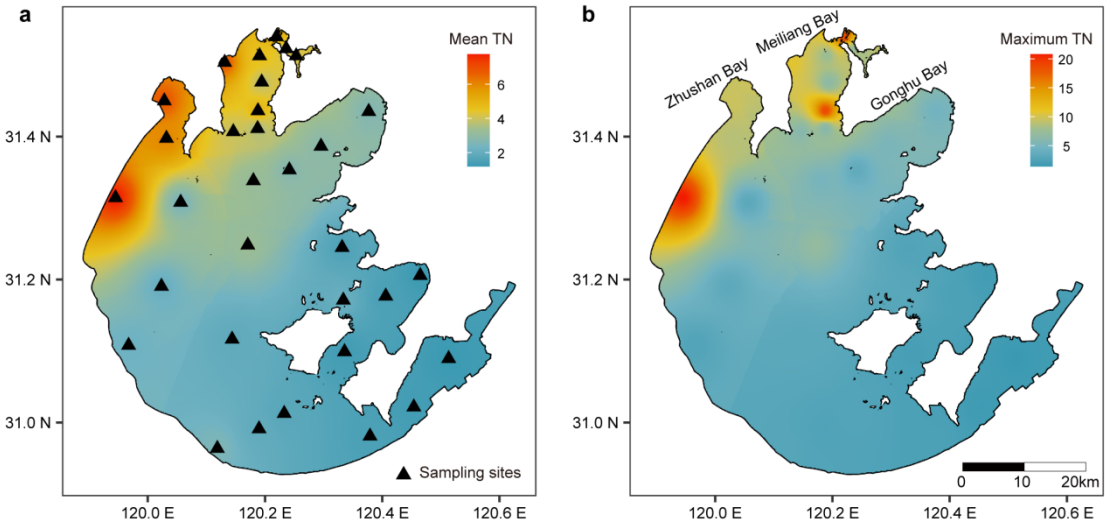

325

326 **Figure S19**. The distribution of mean (a) and maximum (b) total nitrogen (TN)
327 concentrations (mg L^{-1}) in 2007 across the Taihu Lake. Triangles indicate 32 sampling
328 sites.

329

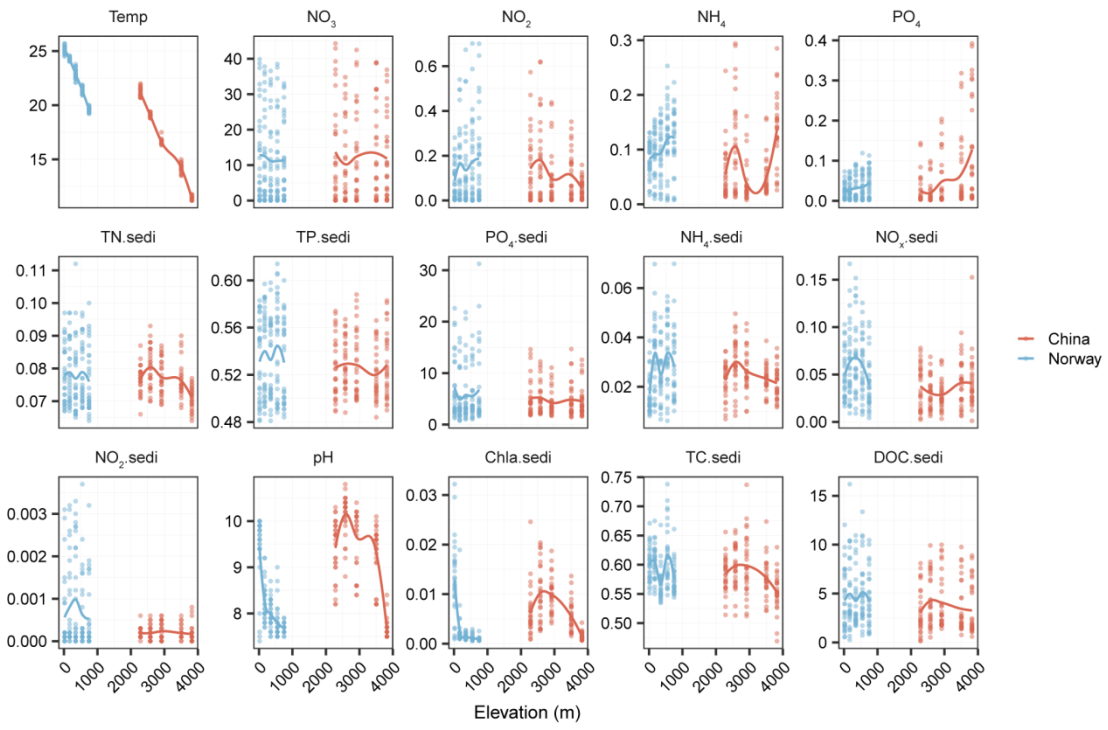

330

331 **Figure S20**. Environmental variables along the elevational gradients, as visualized with
332 loess regression models. The abbreviations of explanatory variables are detailed in Table
333 S1.

334

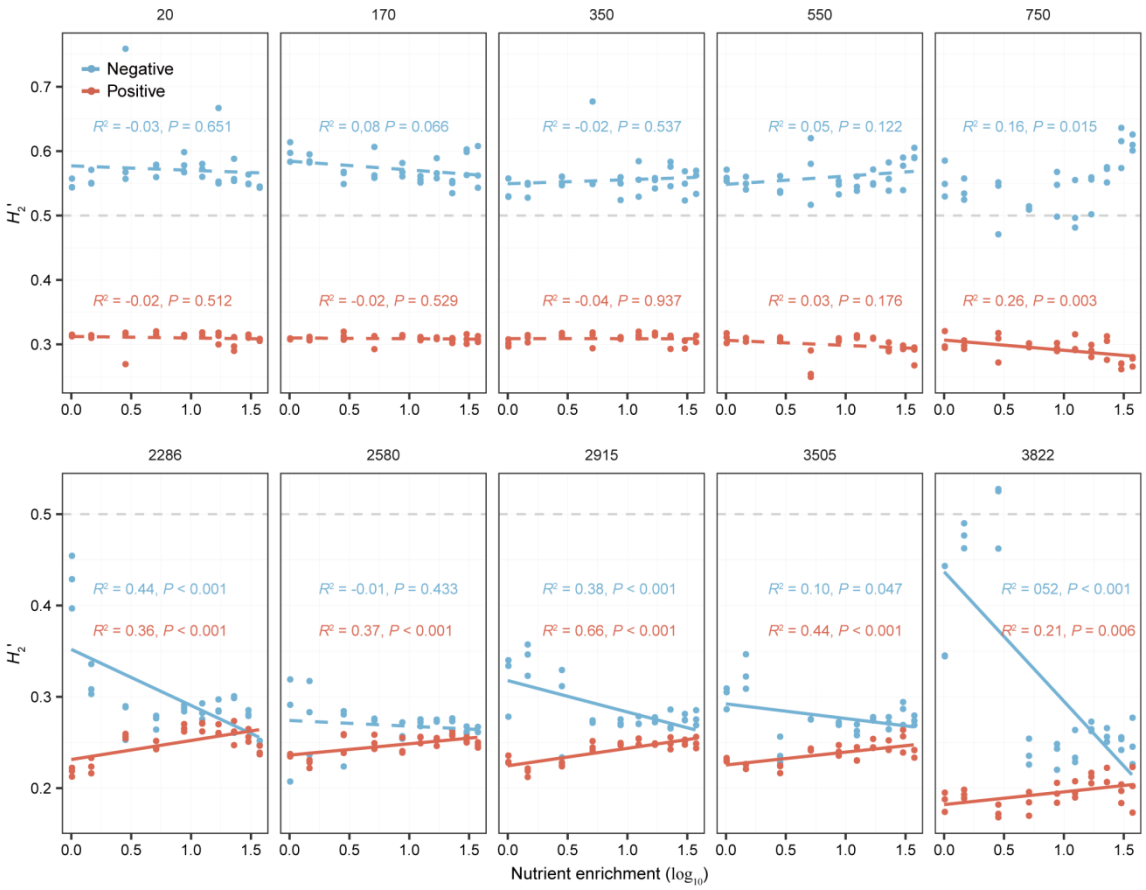

335

336 **Figure S21**. The effects of nutrient enrichment on the observed values of specialization
337 H_2' of DOM-bacteria bipartite networks. We plotted the H_2' against the nutrient gradient
338 of nitrate for both negative (blue lines) and positive (red lines) networks for each
339 elevation in China or Norway, and their relationships are indicated by solid ($P \leq 0.05$) or
340 dotted ($P > 0.05$) lines using linear models with one-sided F-statistics. The horizontal
341 dashed lines indicate more specialized relations with a H_2' value above 0.5.

342

References

1. de Sassi C, Lewis OT, Tylianakis JM. Plant-mediated and nonadditive effects of two global change drivers on an insect herbivore community. *Ecology* 2012, **93**(8)**:** 1892-1901.

2. Glassman SI, Weihe C, Li J, Albright MBN, Looby CI, Martiny AC*, et al.* Decomposition responses to climate depend on microbial community composition. *Proc Natl Acad Sci U S A* 2018, **115**(47)**:** 11994-11999.

3. Wang J, Pan F, Soininen J, Heino J, Shen J. Nutrient enrichment modifies temperature-biodiversity relationships in large-scale field experiments. *Nat Commun* 2016, **7:** 13960.

4. Jessup CM, Kassen R, Forde SE, Kerr B, Buckling A, Rainey PB*, et al.* Big questions, small worlds: microbial model systems in ecology. *Trends in Ecology & Evolution* 2004, **19**(4)**:** 189-197.